Reaction kinetics by mass spectrometry (in the gas phase and in solution)

Ion-molecule reaction

S_N2 reaction: $CH_3Br + Cl^- \rightarrow Br^- + CH_3Cl$

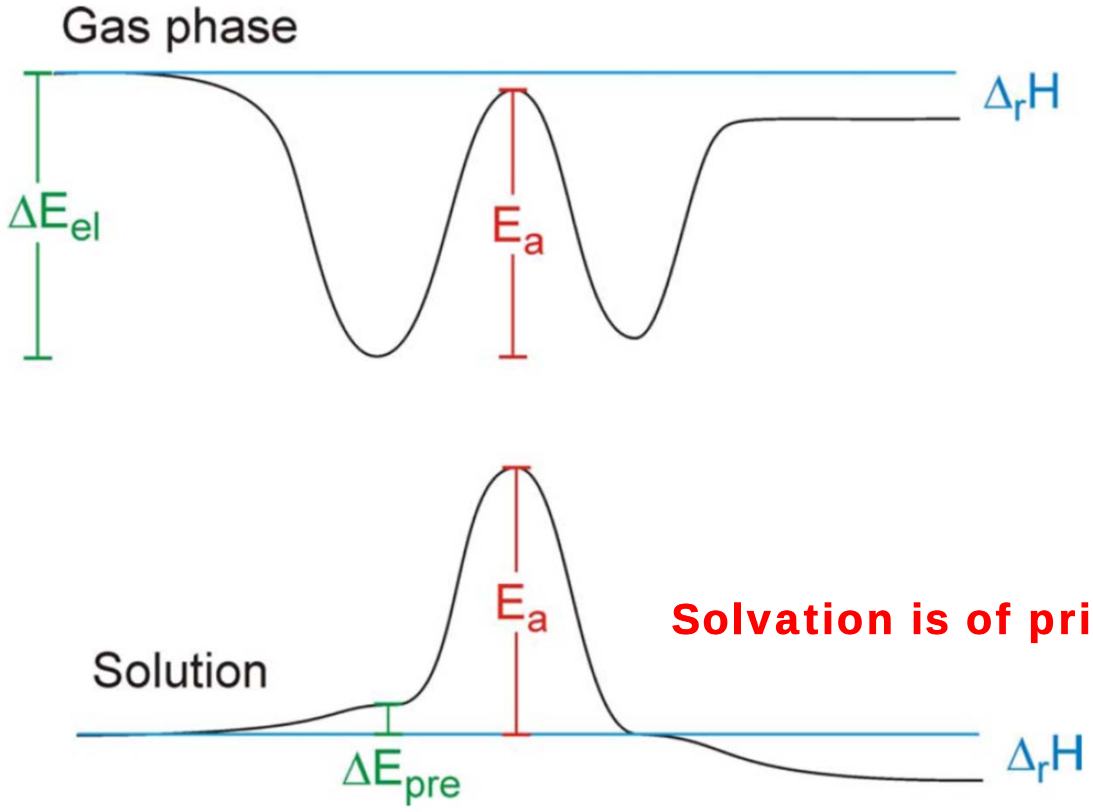

Solvation is of prime importance!

Reactions in the gas phase – tandem in space

$Mg(NO_3)_2$ solution

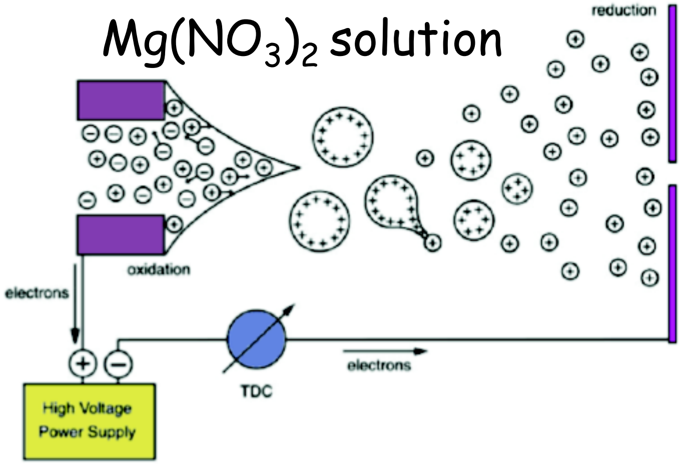

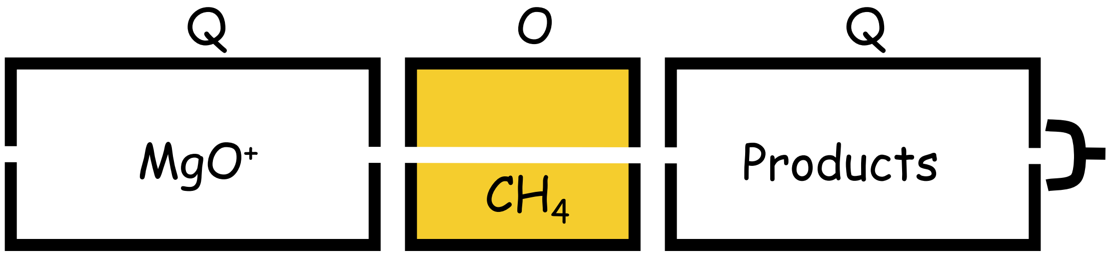

Q	O	Q
MgO^+	CH_4	Products

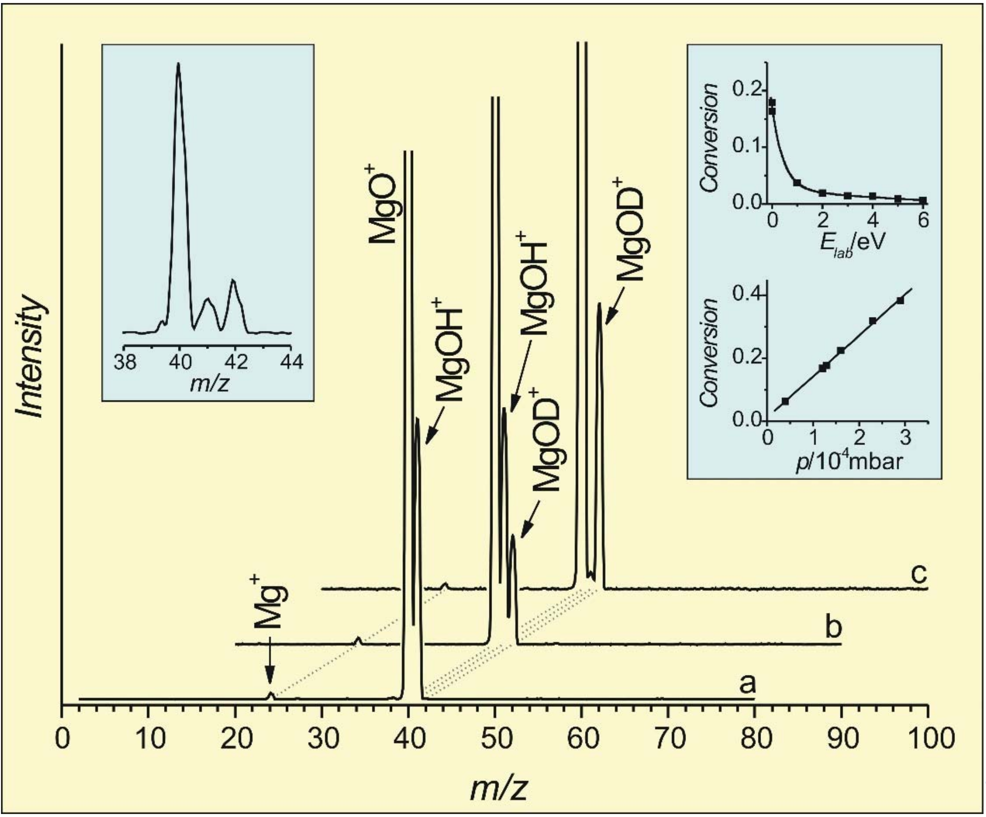

D. Schröder & J. Roithová, *Angew. Chem. Int. Ed.* **2006**, *45*, 5705.

Reactions in the gas phase

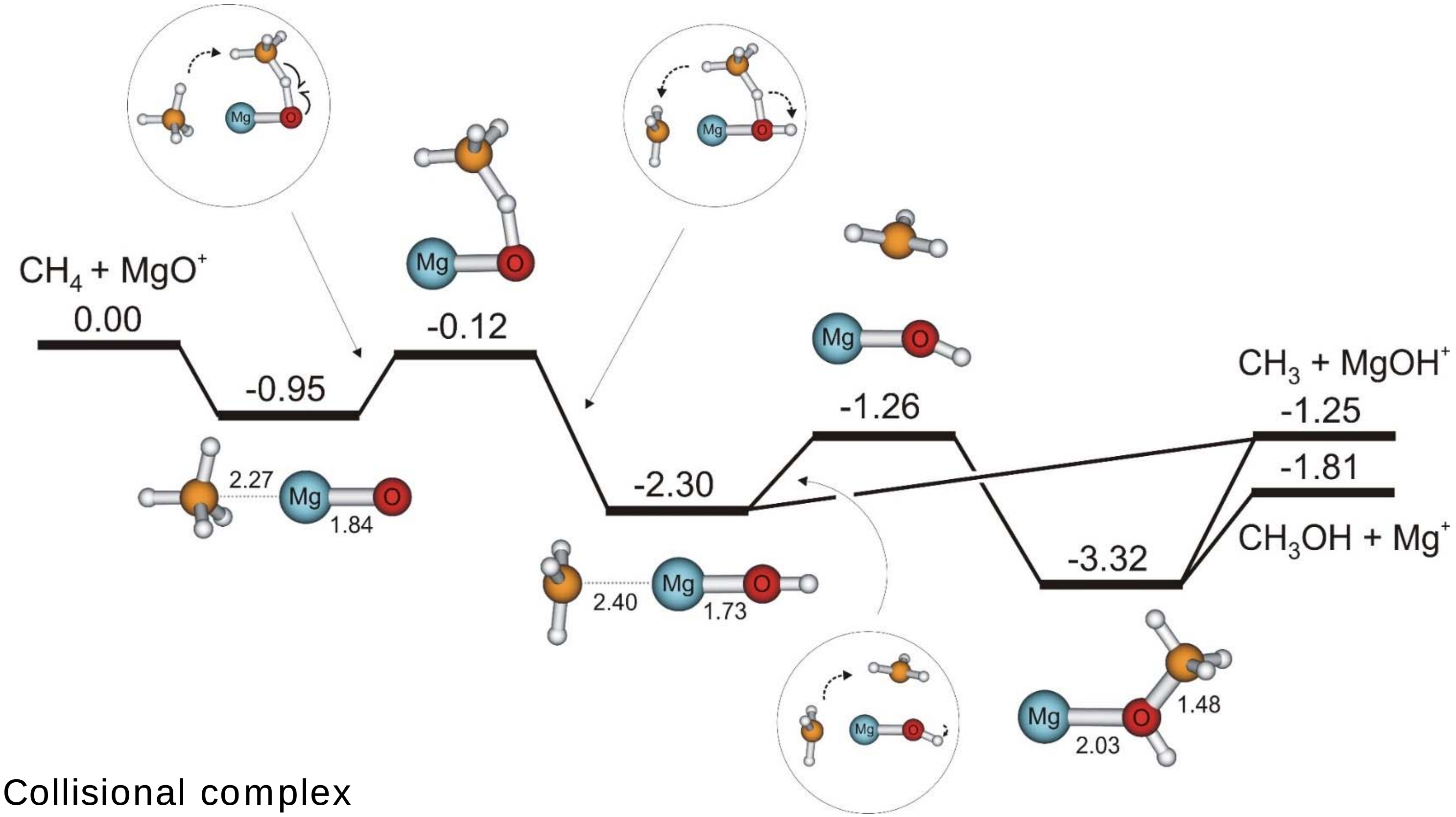

- Collisional complex
- Tight vs. loose transition structure
- Pressure dependence → rate constants

Rate constants (tandem in space)

A → P

1st order kinetics:

$$A = A_0\, e^{-kdt}$$

$$ln\frac{A}{A_0} = -kdt$$

$$d = \frac{p}{k_B T}$$

$$ln\left(1 - \frac{P}{A_0}\right) = -kdt = -k\frac{p}{k_B T}t$$

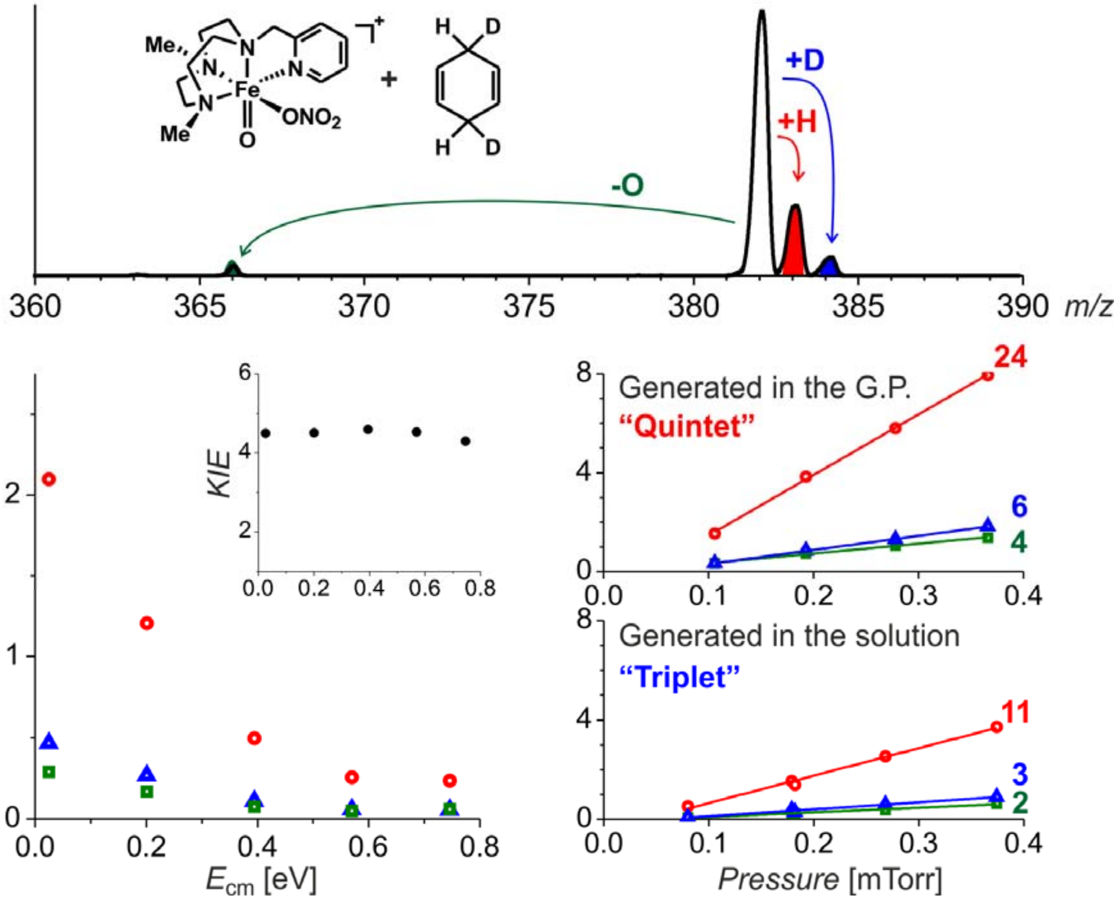

E. Andris et al., *Angew. Chem. Int. Ed.* **2016**, *55*, 3637–3641

Endothermic reactions, reactions with an energy barrier

$C_2H_2^{2+}$ + Ar

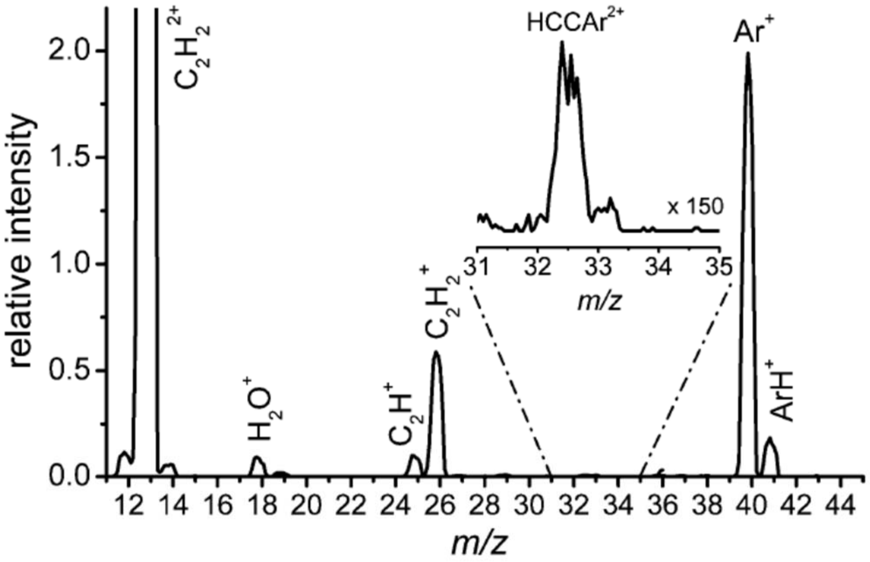

Fig. 1 Reaction of mass-selected $C_2H_2^{2+}$ dications with argon recorded at a collision energy of 4.5 eV in the center-of-mass-frame and with ~2.6×10^{-4} mbar Ar in the reaction cell; the signal intensity of the parent ion (100) is off-scale. The inset shows a mass spectrum of the region of the bond-forming product HCCAr^{2+}, recorded at an Ar-pressure of ~7×10^{-4} mbar, amplified by a factor of 150. The spectrum was recorded with the Trento OQOQ guided-ion beam apparatus.

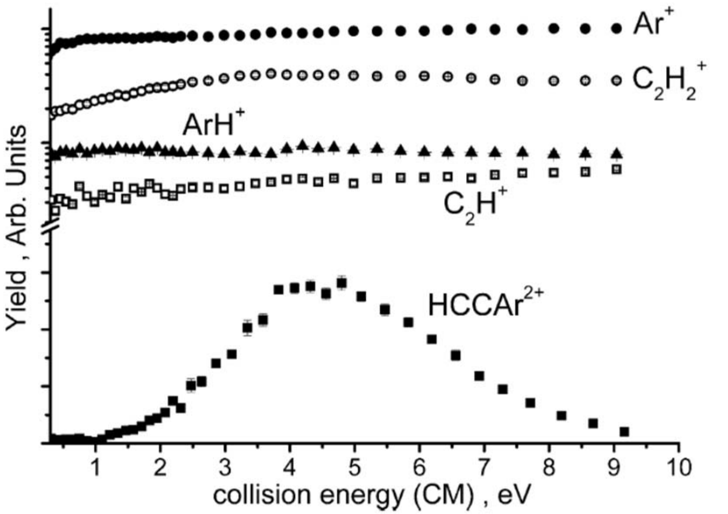

Fig. 2 Yield of ionic products as a function of the collision energy in the reaction of mass-selected $C_2H_2^{2+}$ dications with Ar.

D. Ascenzi et al., *Phys. Chem. Chem. Phys.* **2008**, *10*, 7121.

Reaction dynamics

$C_2H_2^{2+}$ + Ar

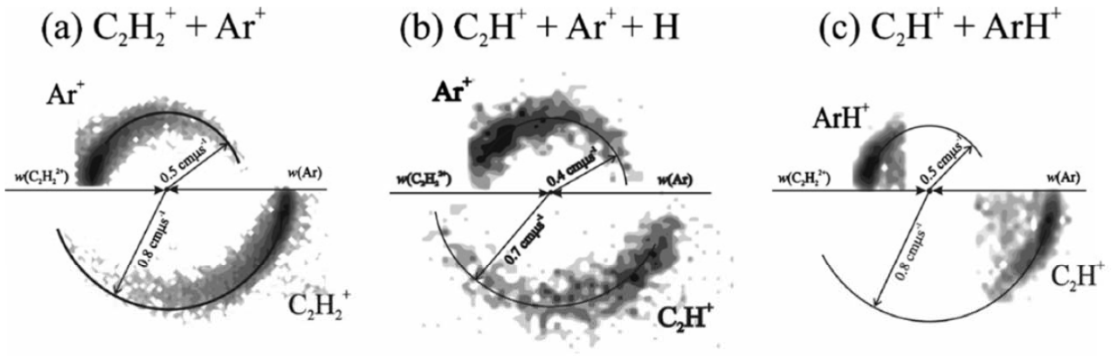

Fig. 4 PSCO scattering diagrams, circle radius as indicated, for the velocities of (a) $C_2H_2^+$ and Ar^+, (b) C_2H^+ and Ar^+, and (c) C_2H^+ and ArH^+ with respect to the center-of-mass velocity of $C_2H_2^{2+}$ for collisions of $C_2H_2^{2+}$ with Ar at E_{CM} = 10.0 eV. Note that the raw experimental data resolves both the scattering angle θ and the azimuthal angle but the scattering data in the figure are summed over the azimuthal angle. Due to the increased volume of this integration as θ increases, the maxima in the scattering diagrams are displaced from $\theta = 0°$ even for a reaction with strongly favored forward scattering.

O_2^{2+} + SCO

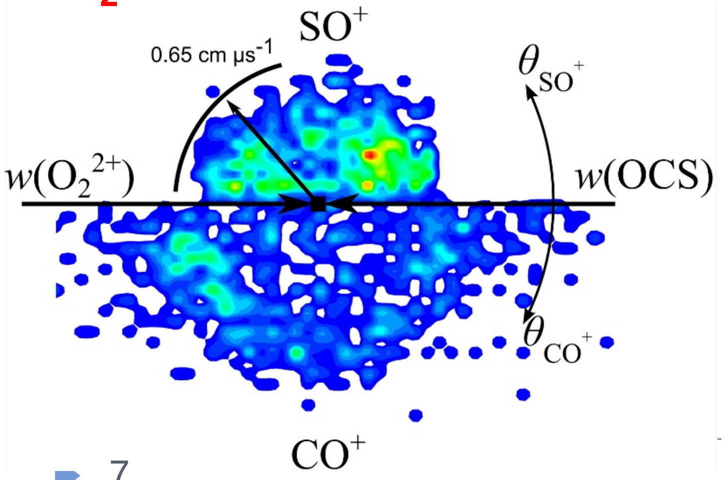

Fig. 1. CM scattering diagram of the SO^+ and CO^+ product ions following the reaction of O_2^{2+} and OCS. The diagram is a polar plot that shows the orientation of the velocities of the SO^+ and CO^+ products with respect to the direction of the reactant velocities, $w(O_2^{2+})$ and $w(OCS)$.

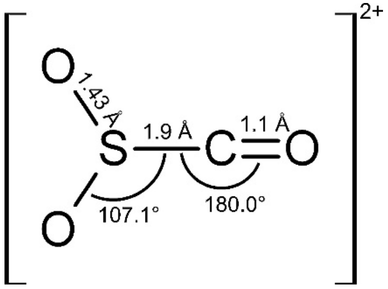

Reaction complex

Reactions in the gas phase – tandem in time

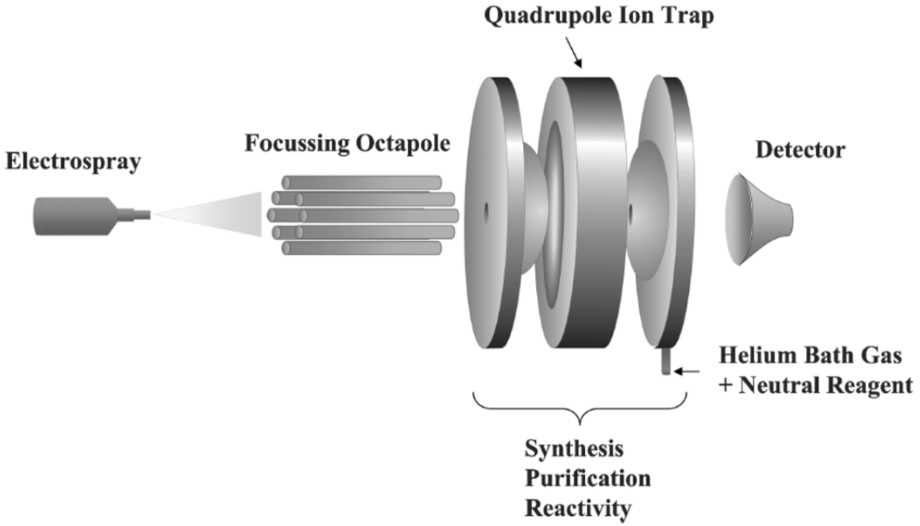

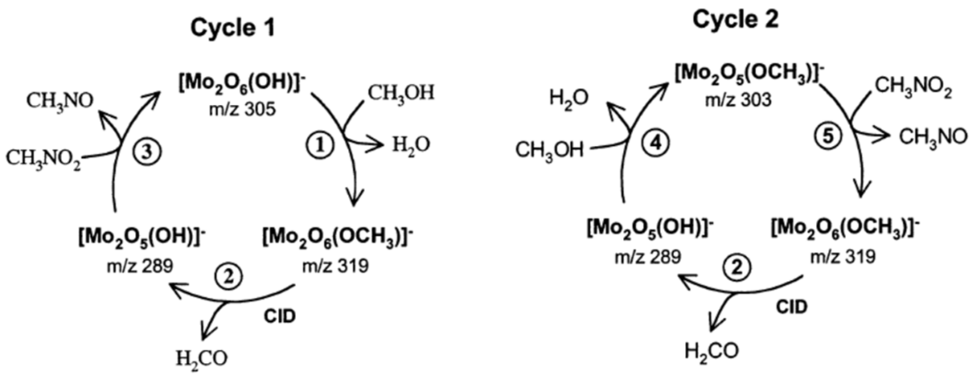

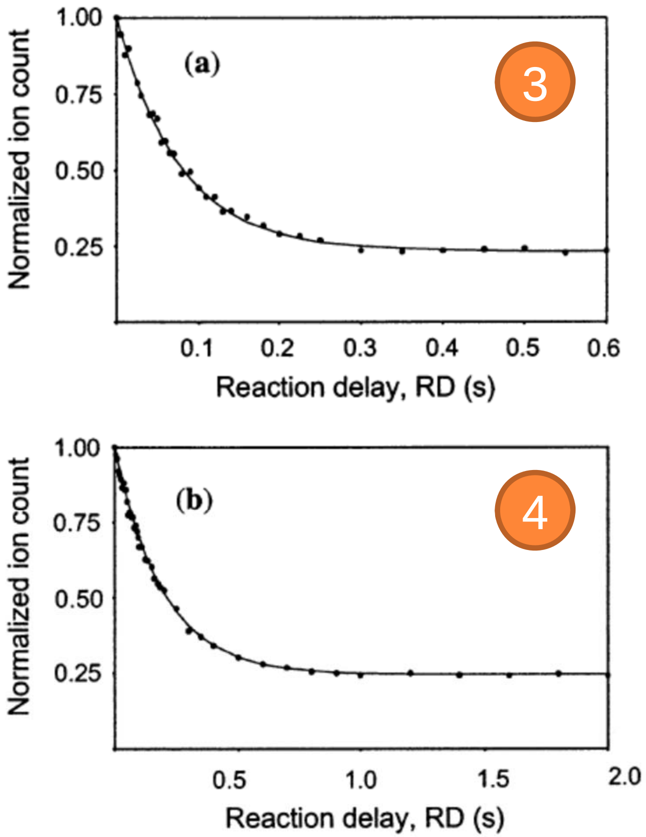

Figure 8. Reaction of $[Mo_2O_5(OH)]^-$ with (**a**) CH_3NO_2 (filled circles) and (**b**) CH_3OH (filled circles). Note the deviation from pesudo first order kinetics in both plots: approximately 20% of the total ion count is unreactive toward both these neutral reagents. The solid lines represent theoretical fits based on the experimentally determined rate constant and amount of unreactive component.

R. A. J. O'Hair, *Chem. Commun.* **2006**, 1469.

Investigation of reactions in solution

- Disappearance of reactants/ appearance of products
- NMR
- GC
- UV/vis
- IR
- MS

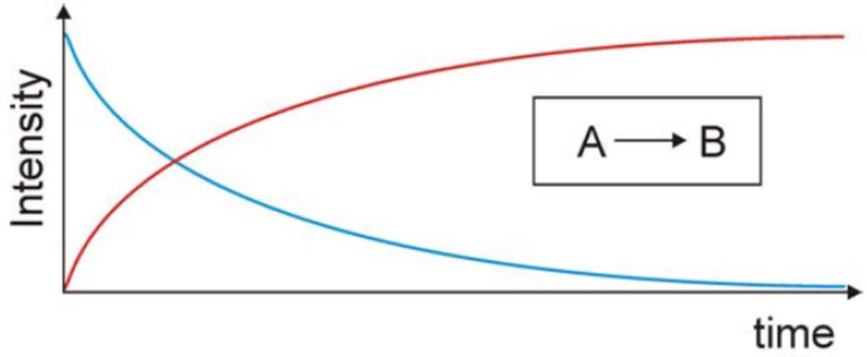

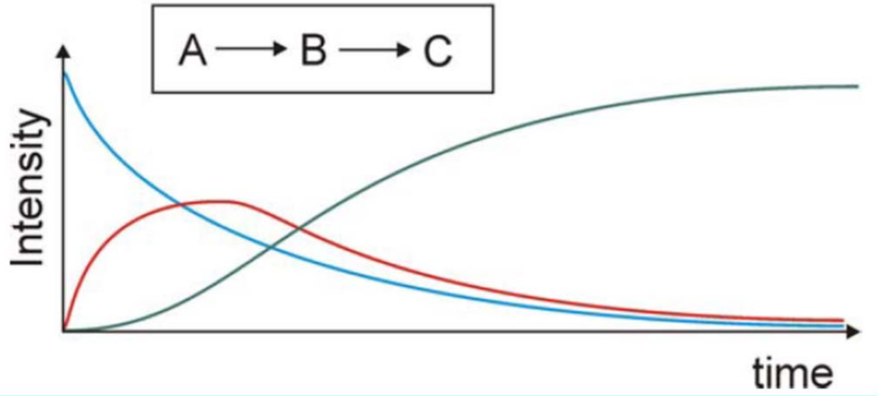

ESI-MS monitoring of solution chemistry

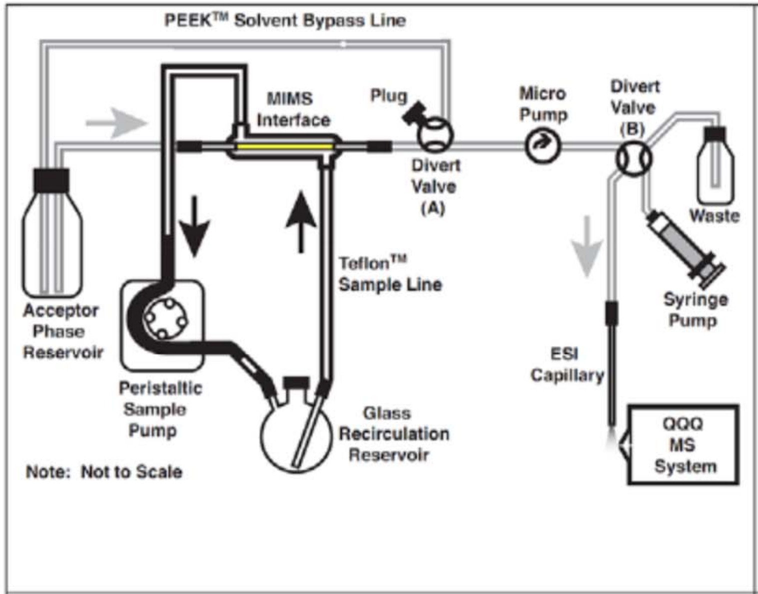

A: Condensed-phase membrane introduction mass spectrometry interface (Reproduced from Duncan (2011), with permission from Wiley Inc ©2011)

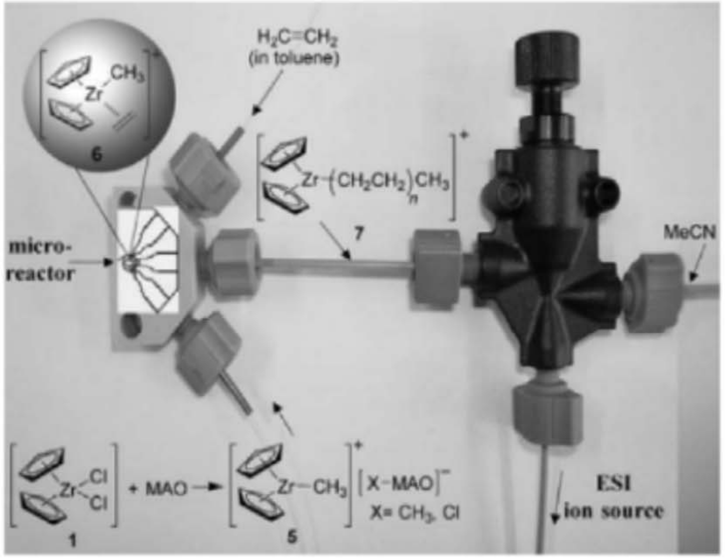

B: Micro-reactor interfaced to mass spectrometry (Reproduced from Santos & Metzger (2006), with permission from Wiley-VCH Verlag GmbH & Co Inc ©2006)

ESI-MS monitoring of solution chemistry

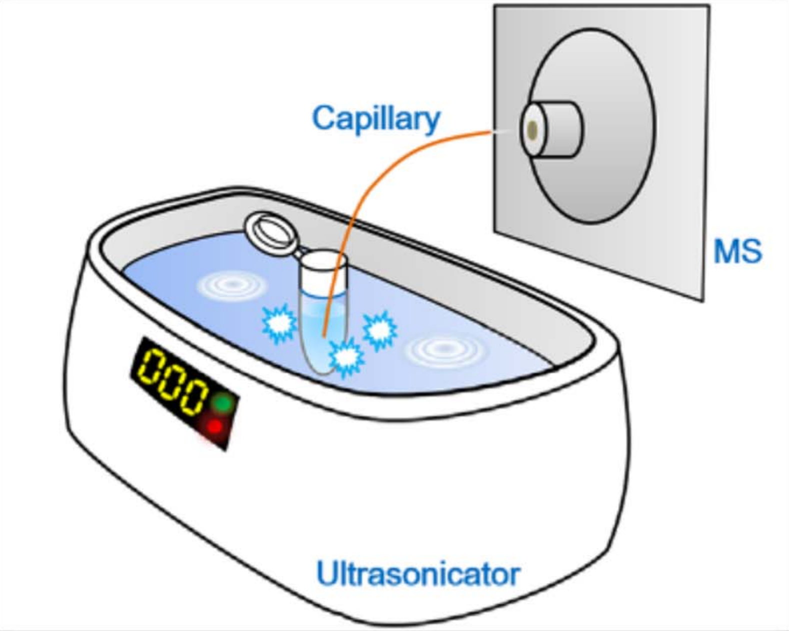

E: Ultrasonication assisted reactions (Reproduced from Chen, Chao (2010), with permission from Royal Society of Chemistry ©2010)

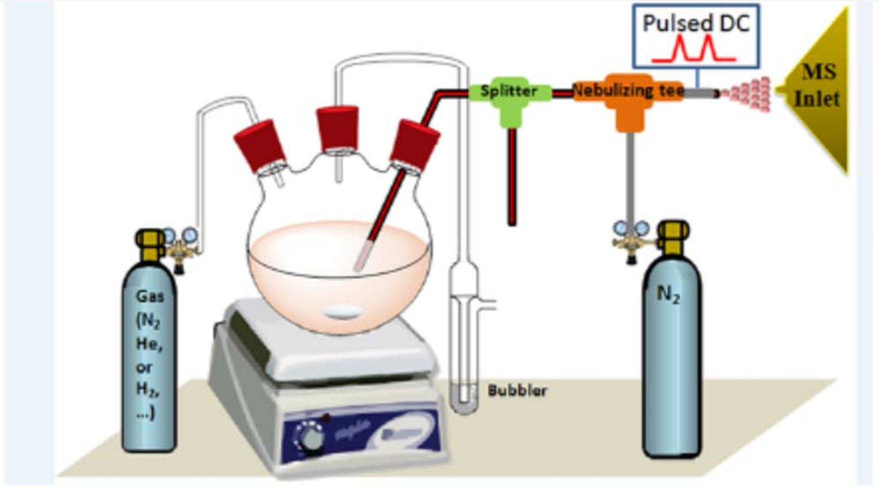

F. Inductive ESI-MS on-line reaction monitoring system (Reproduced from Yan (2014), with permission from Wiley-VCH Verlag GmbH & Co Inc ©2014)

Pressure gap in reaction mechanisms’ research using MS

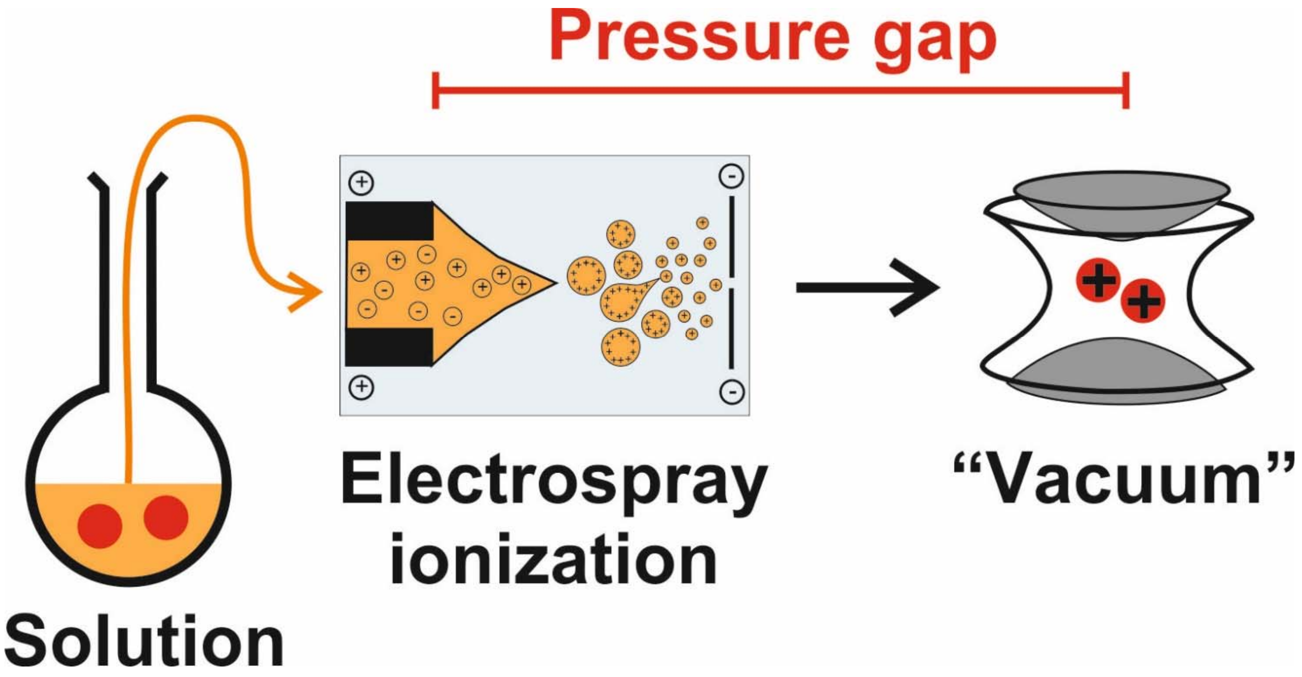

ESI-MS monitoring of solution chemistry

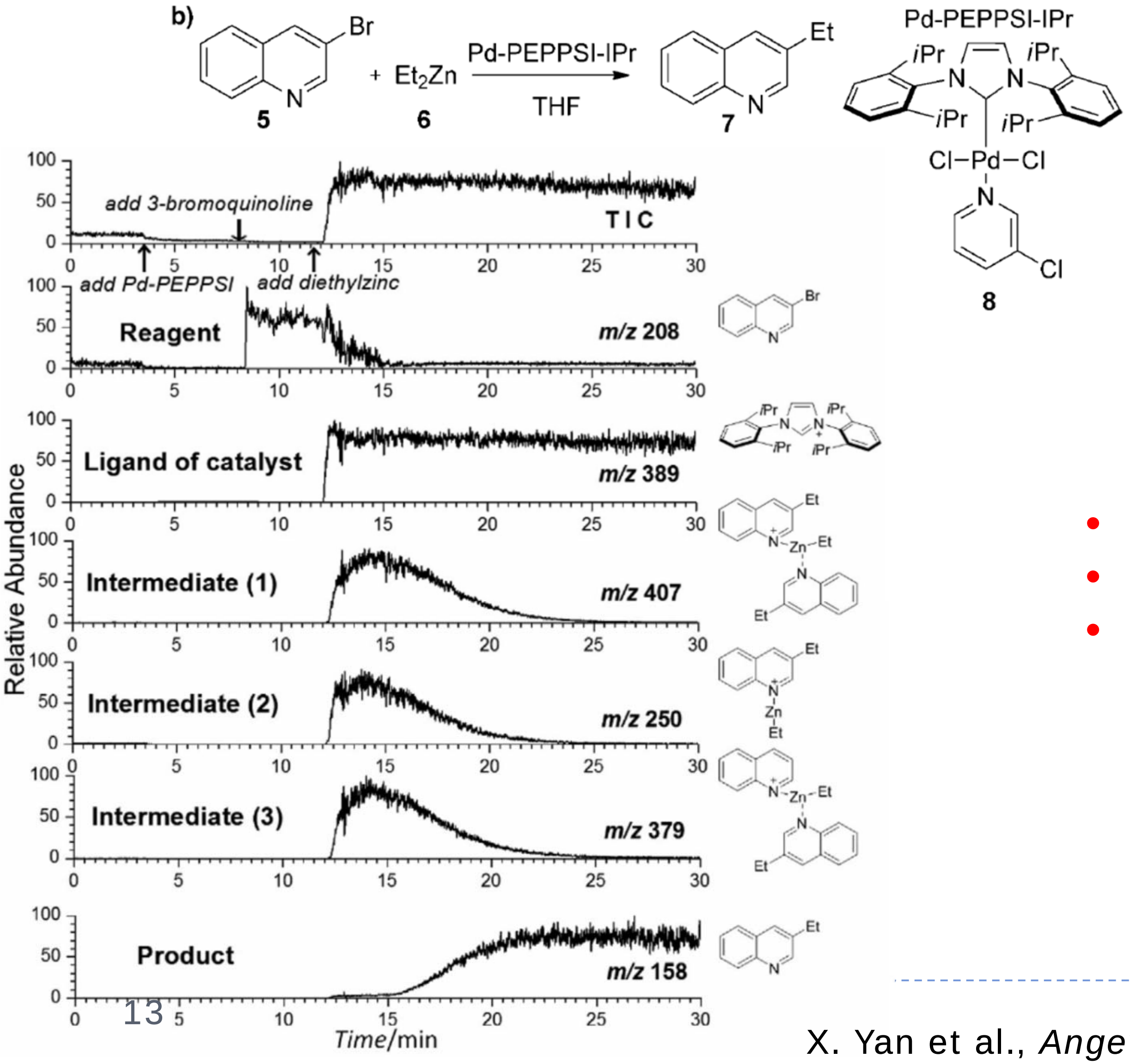

- Ion suppression?
- Linear response?
- Speciation?

X. Yan et al., *Angew. Chem. Int. Ed.* **2014**, *53*, 5931.

Ion response

Dependence on the flow rate

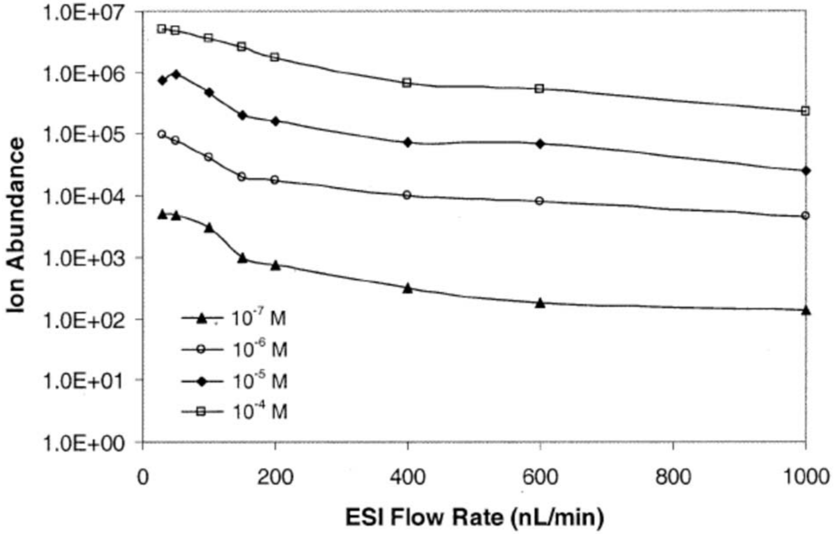

Figure 2. Ion abundance versus electrospray flow rate (in the semi log scale) for reserpine at different solution concentrations.

Relative ion intensities in dependence of concentration → differences larger at large concentrations

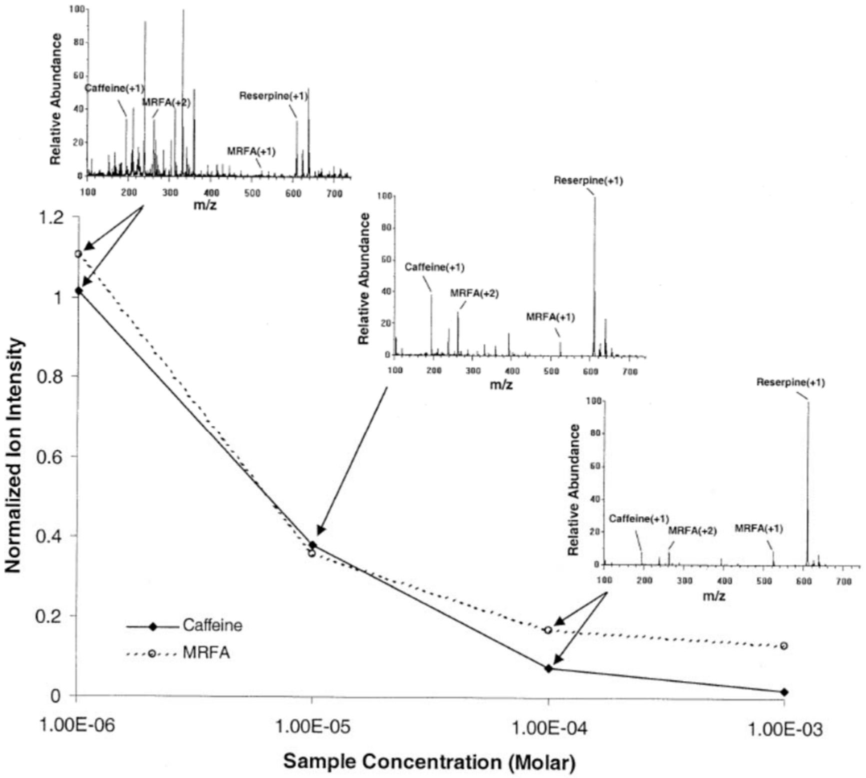

Figure 4. Normalized ion intensities of caffeine (195.1^{+}) and MRFA (524.4^{+}, 262.7^{++}) to the intensity of the reserpine (609.2^{+}) peak at different mixture concentrations. Representative mass spectra for the three lesser concentrations are also shown. Electrospray flow rate: 1 μl/min.

Sometimes linear ESI-MS response

- **Streptavidin + biotin**

$$(S_4 + iB) + B \underset{k_{off,(i+1)}}{\overset{k_{on,i}}{\rightleftarrows}} (S_4 + (i+1)B)$$

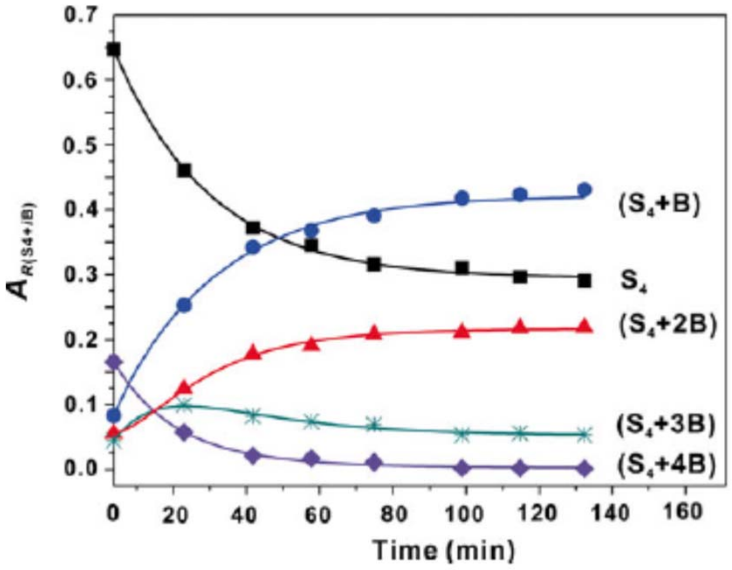

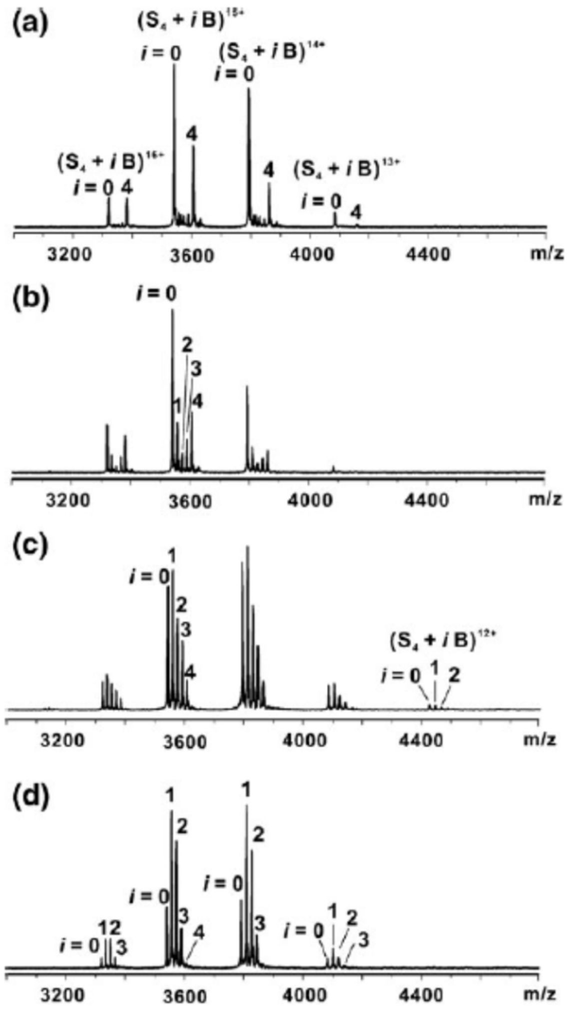

Lu Deng et al., *J. Am. Soc. Mass Spectrom.* **2013**, *24*, 49.

Usually, only qualitatively

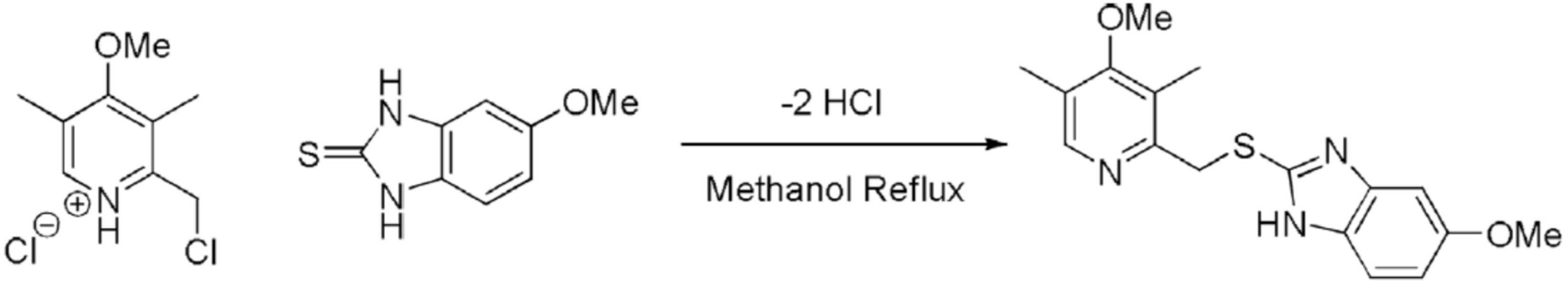

NMR

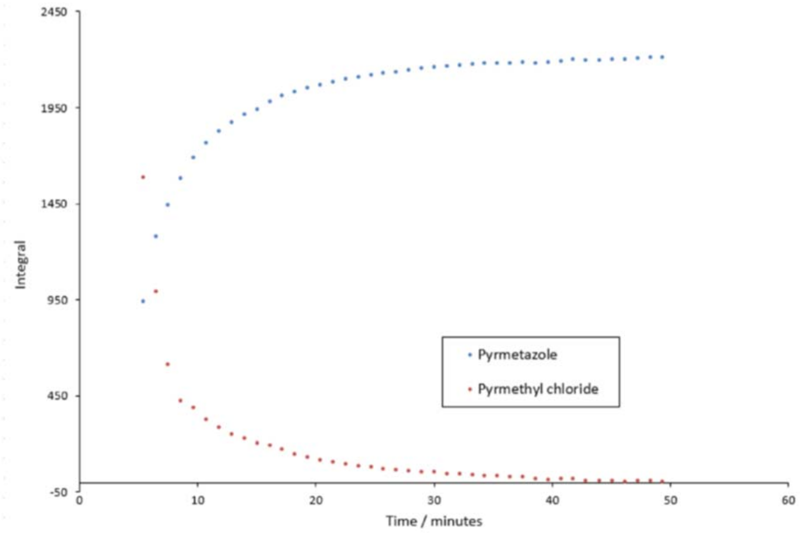

ESI-MS

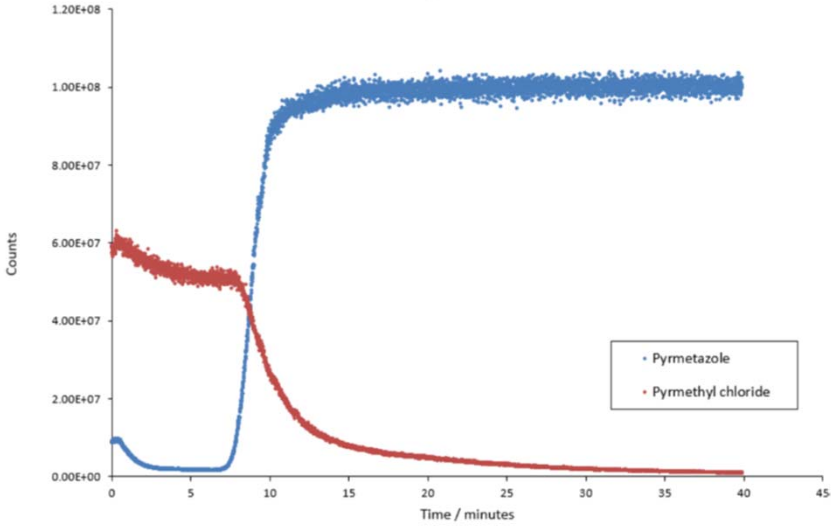

A. Ray et al., *Mass Spec Rev.* **2018**, *37*, 565.

Reactions in droplets during ESI

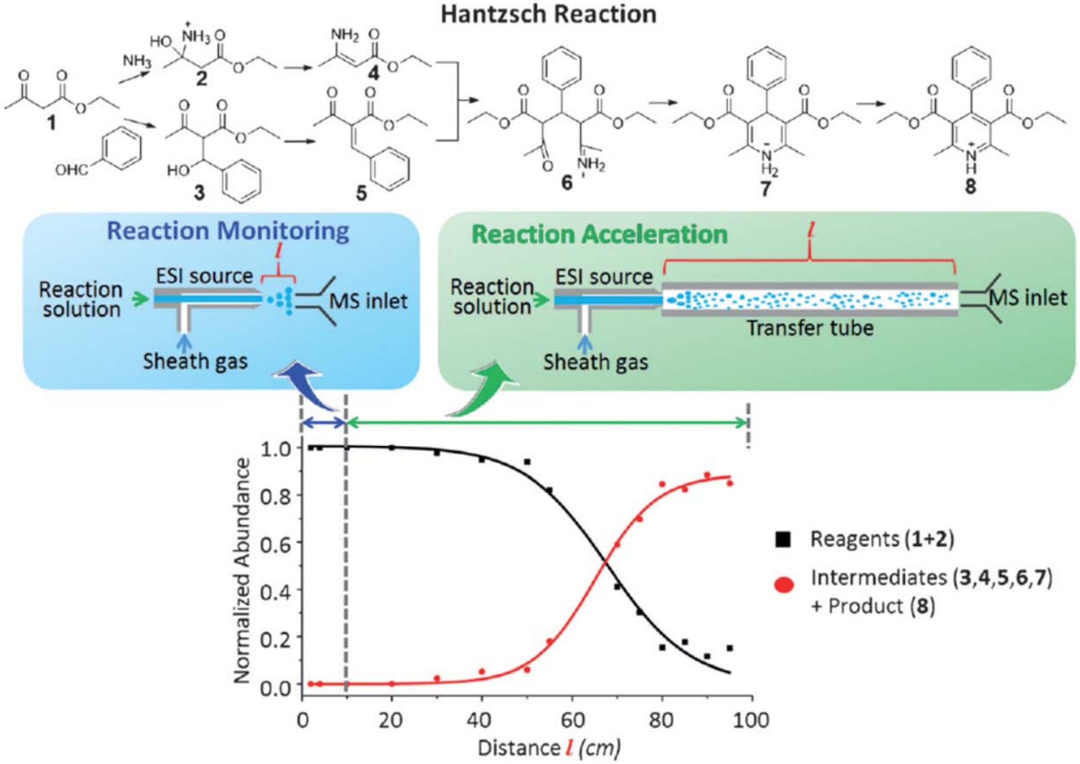

Figure 1. Reaction monitoring versus reaction acceleration of the Hantzsch reaction in electrospray droplets as a function of the distance (*l*) between the MS inlet and the spray source. The transfer tube was simply used to focus droplets in the reaction-acceleration experiments. The dotted line indicates the safe distance for doing reaction monitoring before acceleration starts in this specific example.

- All condensation reactions will be accelerated!
- Concentration of metal catalysts will significantly increase!

Xin Yan, Ryan M. Bain, and R. Graham Cooks, *Angew. Chem. Int. Ed.* **2016**, *55*, 12960.

Reactions in droplets

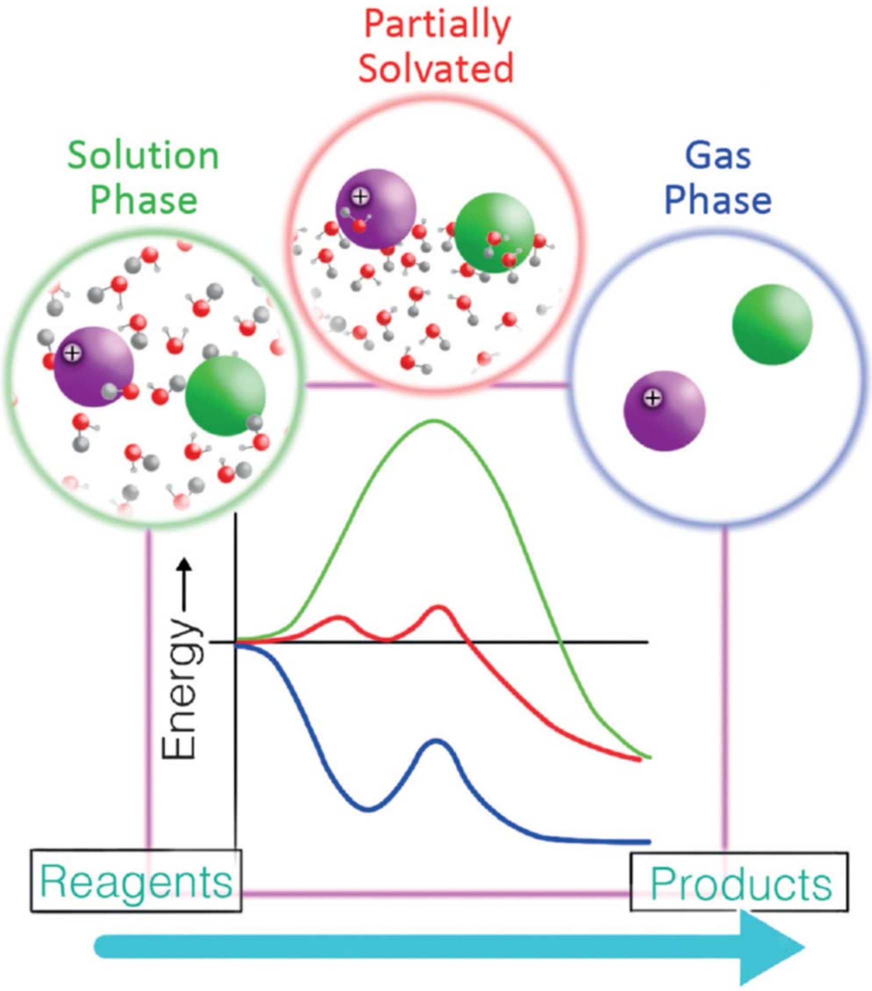

Figure 10. Energetics associated with incomplete solvation underlies acceleration of reactions occurring at the interface. The bulk solution phase reaction has a substantial energetic (and free energy) barrier; the gas phase ion/molecule reaction occurs on every collision while the droplet reaction occurs at an accelerated rate compared to bulk and in a fashion which increases with the surface/volume ratio, viz. in small droplets.

Xin Yan, Ryan M. Bain, and R. Graham Cooks, *Angew. Chem. Int. Ed.* **2016**, *55*, 12960.

Reactions in droplets

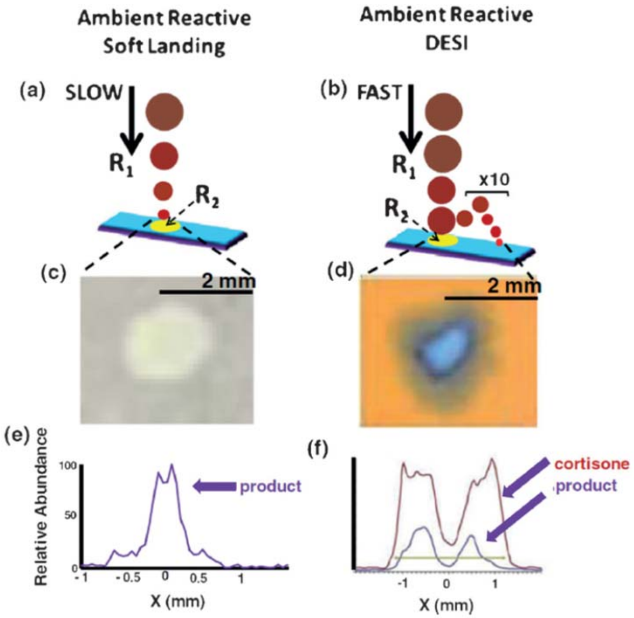

Figure 6. Contrasting reaction-product distributions obtained upon impact of electrospray droplets using a) an ambient soft landing apparatus, utilizing low-velocity droplets or b) DESI, with high-velocity droplets. Soft landing yields product spots in which the product ions (*m*/*z* 474) are concentrated at the centers (c), whereas in the DESI experiment, the products are found in a splash ring surrounding the impact point (d,f). Reproduced from Ref. [14a] with permission from Springer.

Going preparative?

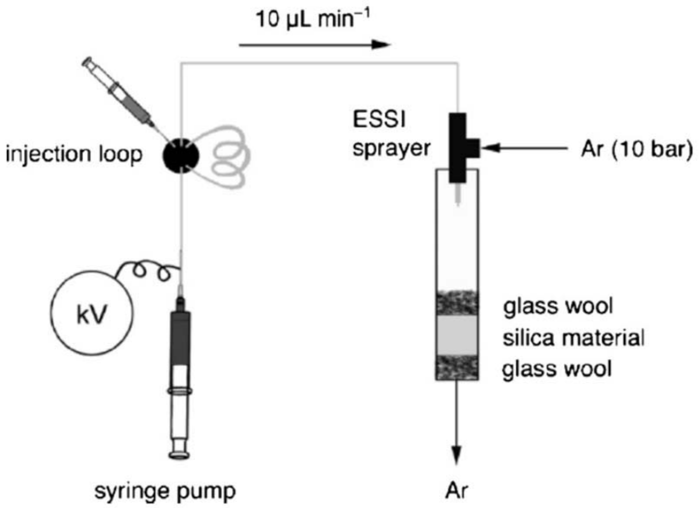

Figure 9. Synthesis using an electrosprayer enclosed in a polypropylene vessel with a collecting surface of glass wool and silica. The high voltage was applied through the stainless steel needle of the syringe while a grounded aluminum foil covered the vessel. Reproduced from Ref. [15] with permission from John Wiley and Sons.

Reactions occur in secondary (splashed) droplets

Concentration changes

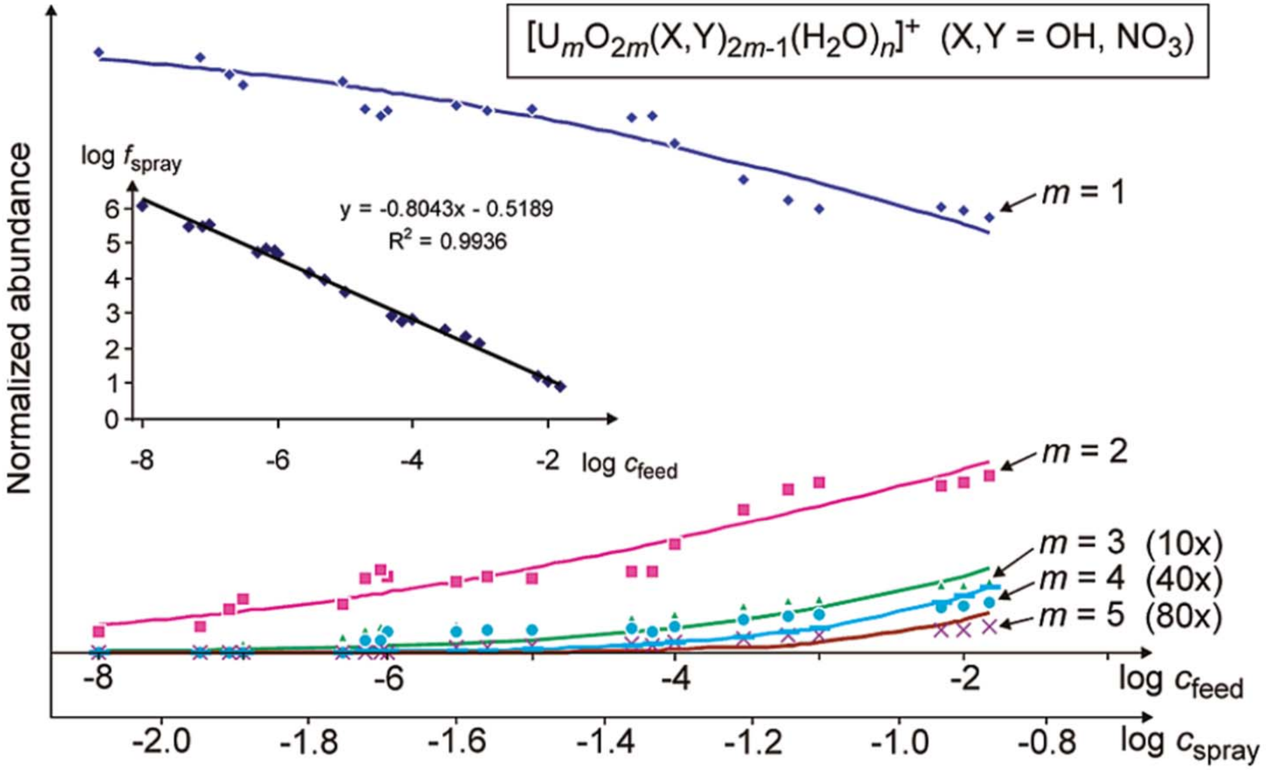

Figure 6. Normalized ion abundances of the mono- and oligonuclear species $[U_mO_{2m}(X,Y)_{2m-1}(H_2O)_n]^+$ (X, Y = OH, NO_3) in the ESI mass spectra of $UO_2(NO_3)_2$ in water as a function of the concentration of the feed solutions (c_{feed}) of the ESI source and the derived concentration in the electrospray process (c_{spray}).

f_{spray} – enrichment factor during ESI → depending on concentration,

$f_{spray} \rightarrow 10^6$

N. G. Tsierkezos et al., *Inorg. Chem.* **2009**, *48*, 6287.

Kinetics directly

Scheme 1. Speciation of Allylindium Halides in Solution[a]

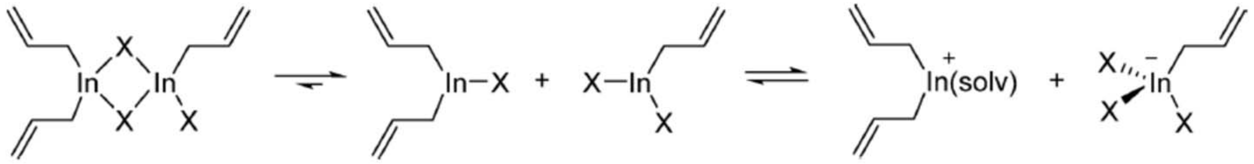

[a]X = Br, I. For simplicity, coordinating solvent molecules are omitted for neutral indium centers.

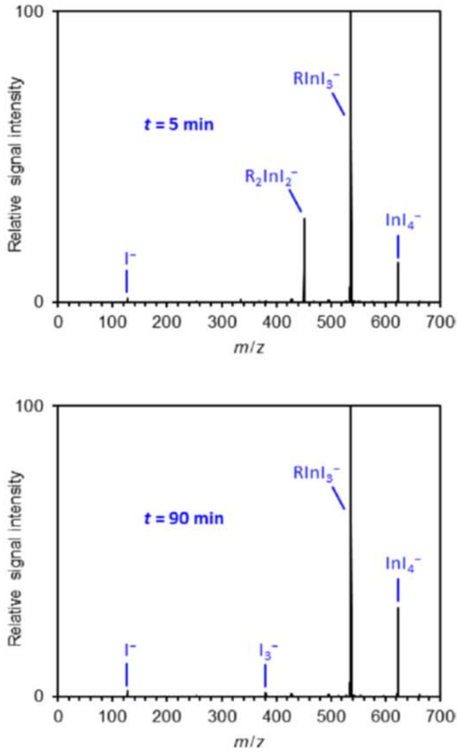

Figure 2. Negative-ion mode ESI mass spectra of a solution of formal $R_3In_2I_3$ in D_2O: (top) 5 min after sample preparation and (bottom) 90 min after sample preparation (R = allyl).

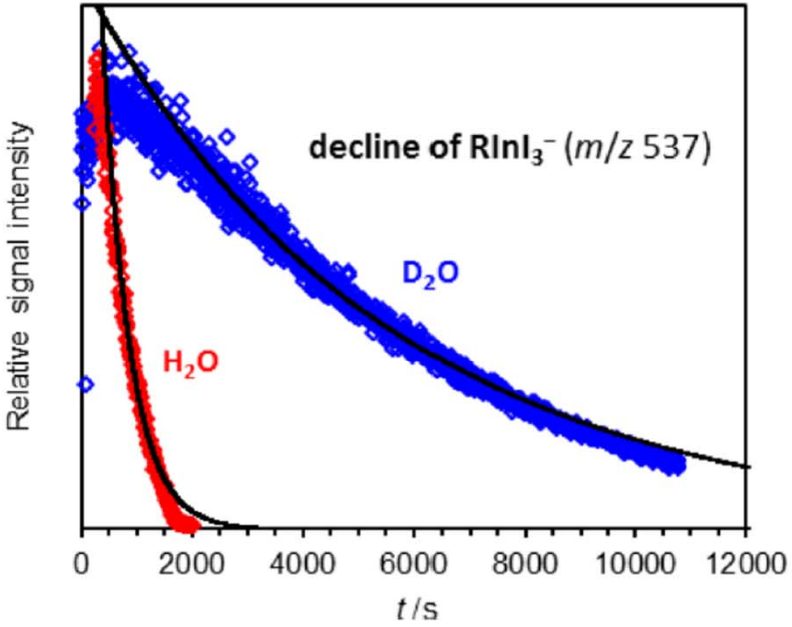

K. Koszinowski, D. S. Stephenson, *J. Org. Chem.* **2018**, *83*, 14314

Kinetics directly

Scheme 1. Speciation of Allylindium Halides in Solution[a]

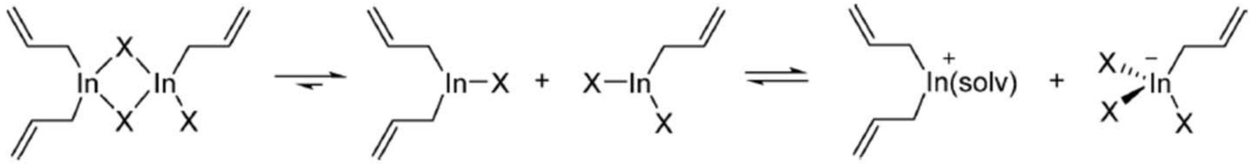

[a] X = Br, I. For simplicity, coordinating solvent molecules are omitted for neutral indium centers.

ESI-MS

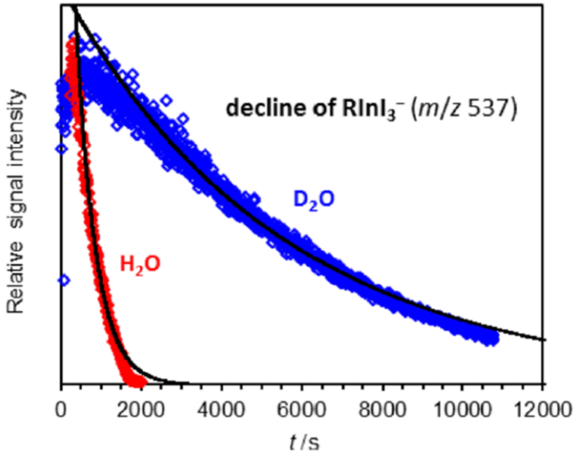

NMR

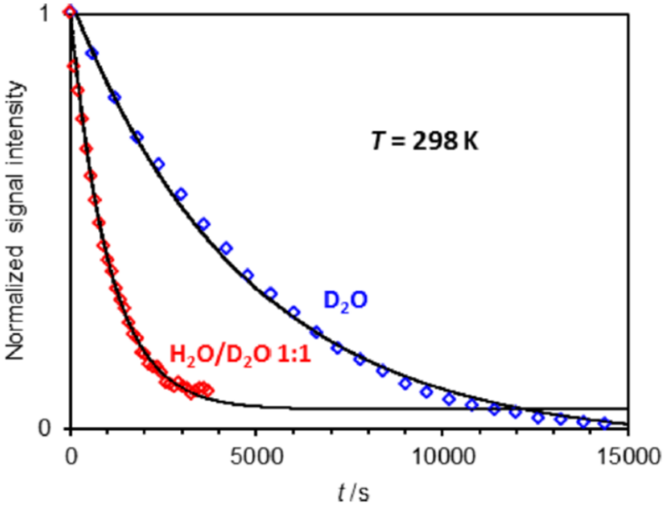

Figure 6. Time profiles of the ^1H NMR signal intensities of formal $R_3In_2I_3$ in D_2O (blue symbols) and a 1:1 mixture of H_2O and D_2O (red symbols) at 298 K together with monoexponential fits (black lines, R = allyl).

K. Koszinowski, D. S. Stephenson, *J. Org. Chem.* **2018**, *83*, 14314

Reactive intermediates, metal complexes, organometallic compounds

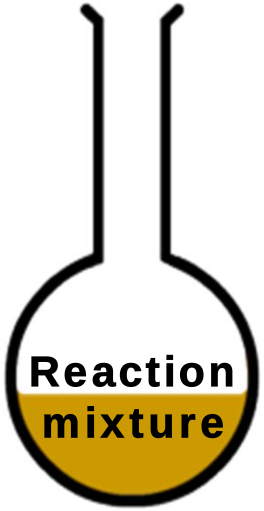

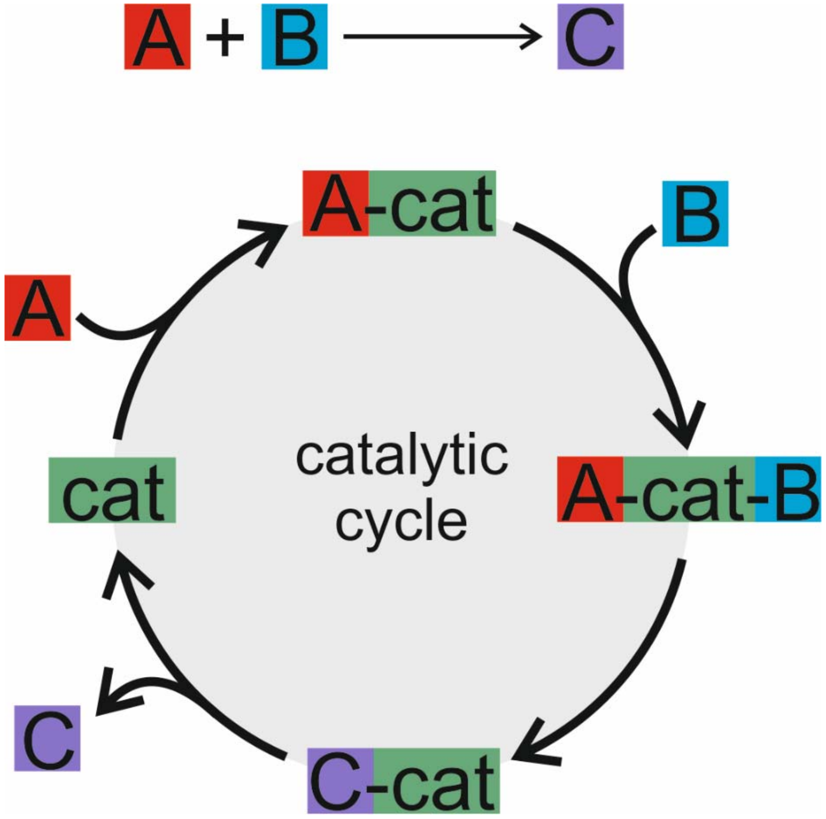

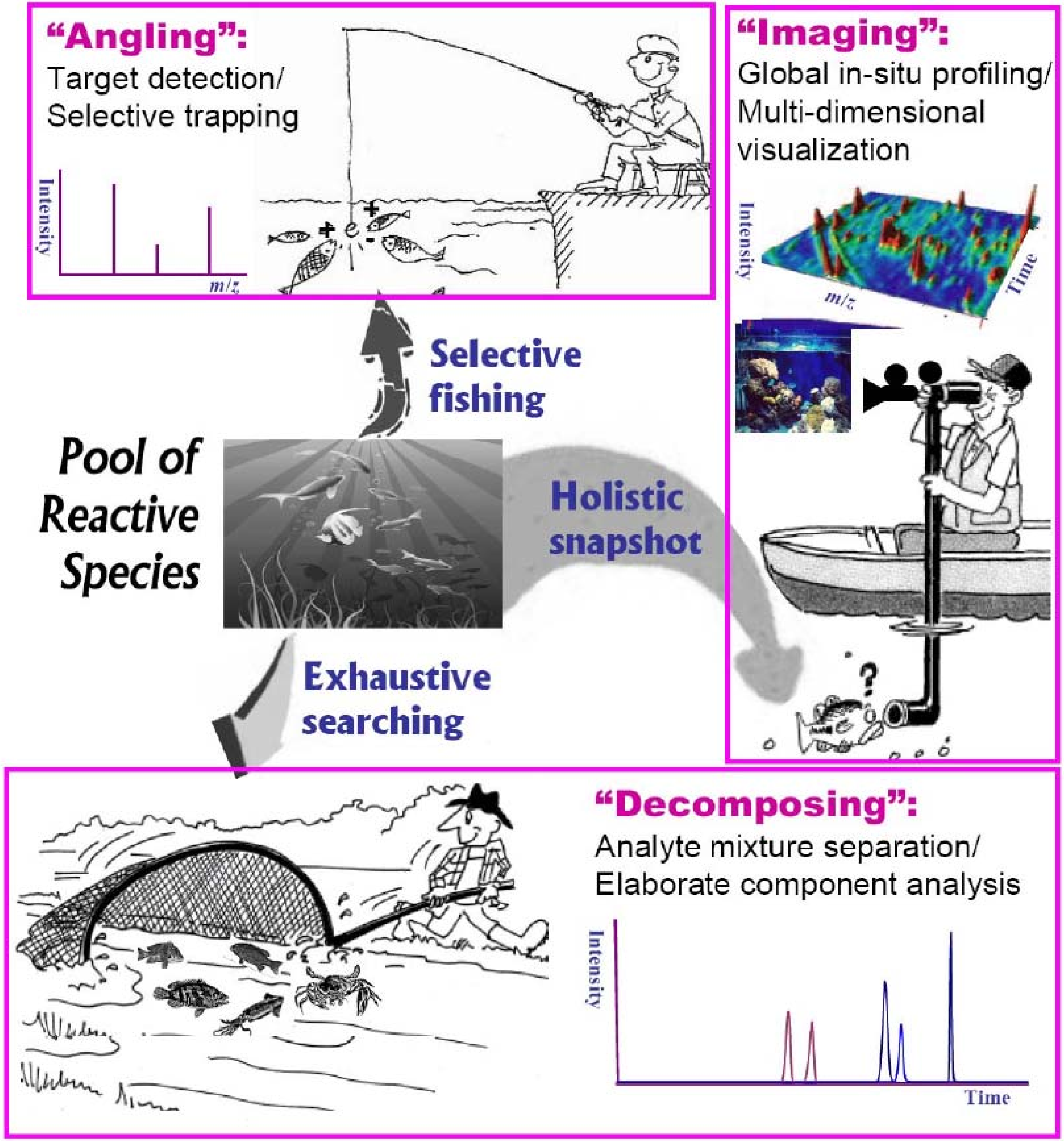

"Angling":
Target detection/
Selective trapping

"Imaging":
Global in-situ profiling/
Multi-dimensional
visualization

Selective fishing

Pool of Reactive Species

Holistic snapshot

Exhaustive searching

"Decomposing":
Analyte mixture separation/
Elaborate component analysis

Reaction mechanisms research

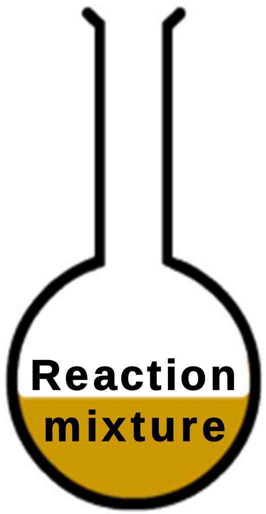

$A + B \longrightarrow C$

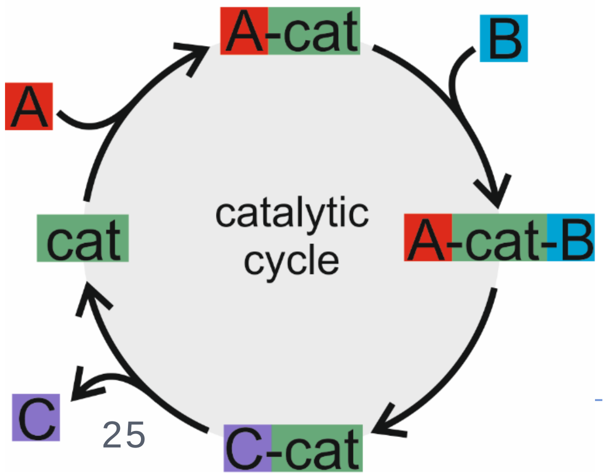

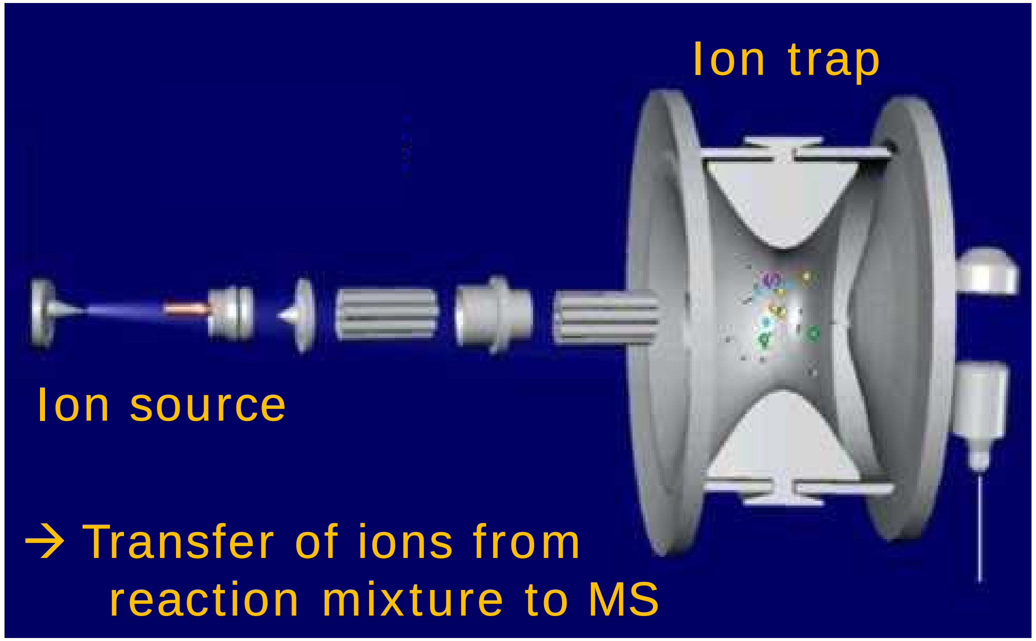

→ Transfer of ions from reaction mixture to MS

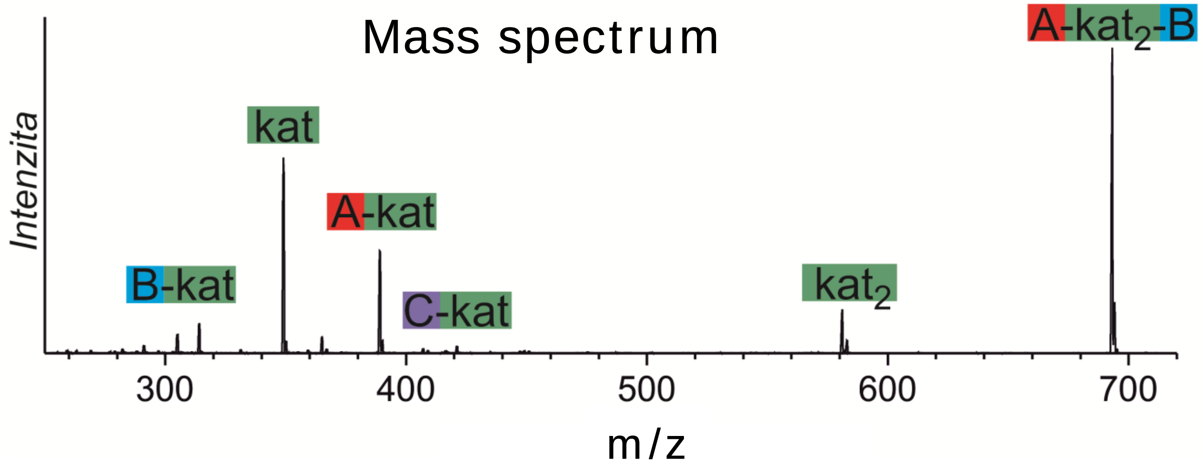
Mass spectrum

Isotope dilution mass spectrometry

- Quantification by MS → using isotopically labelled standards
- Quantification of metabolites by ESI-MS:

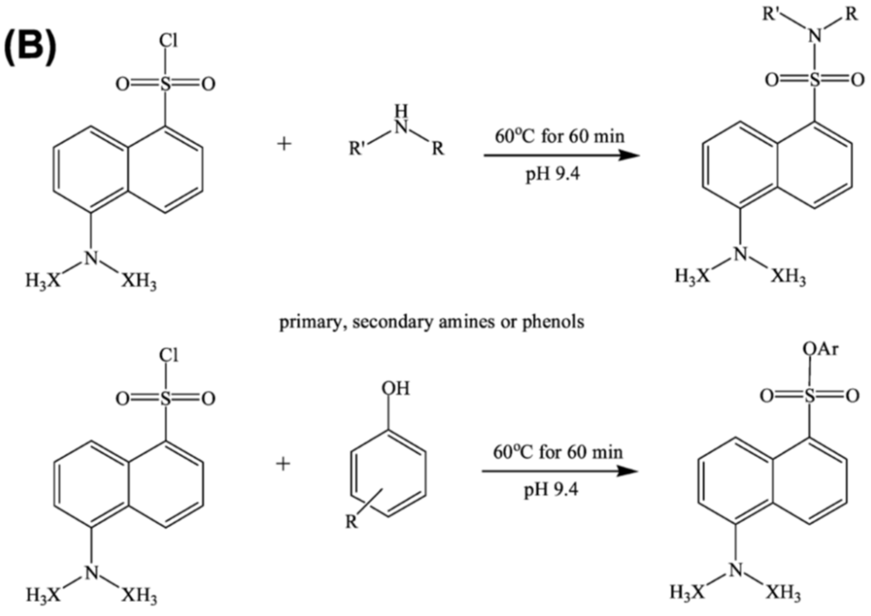

X = ^{12}C: dansyl chloride
X = ^{13}C: ^{13}C-dansyl chloride

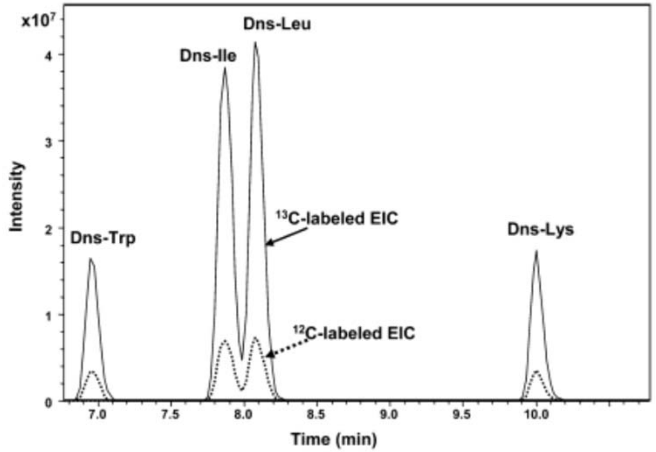

Figure 3. Extracted ion chromatograms of 1:5 of ^{12}C-/^{13}C-dansylated Trp, Ile, Leu, and Lys obtained by fast gradient RPLC/FTICR MS.

K. Guo, L. Li, *Anal. Chem.* **2009**, *81*, 3919.

J.I. Garcia Alonso, P. Rodriguez-Gonzalez, Isotope dilution mass spectrometry, Royal Society of Chemistry, 2013, Cambridge (UK).

Dynamic isotope dilution for kinetic measurement: Delayed Reactant Labelling

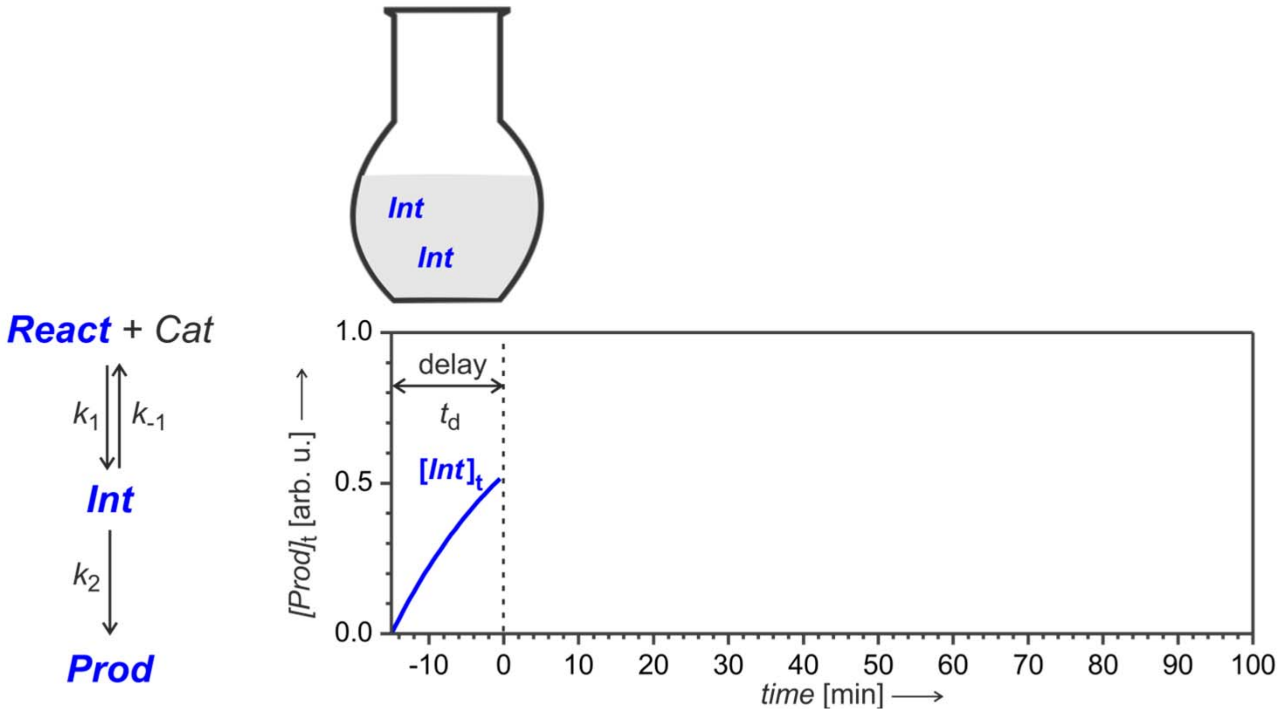

L. Jašíková, M. Anania, S. Hybelbauerová, J. Roithová, *J. Am. Chem. Soc.* **2015**, *137*, 13647.

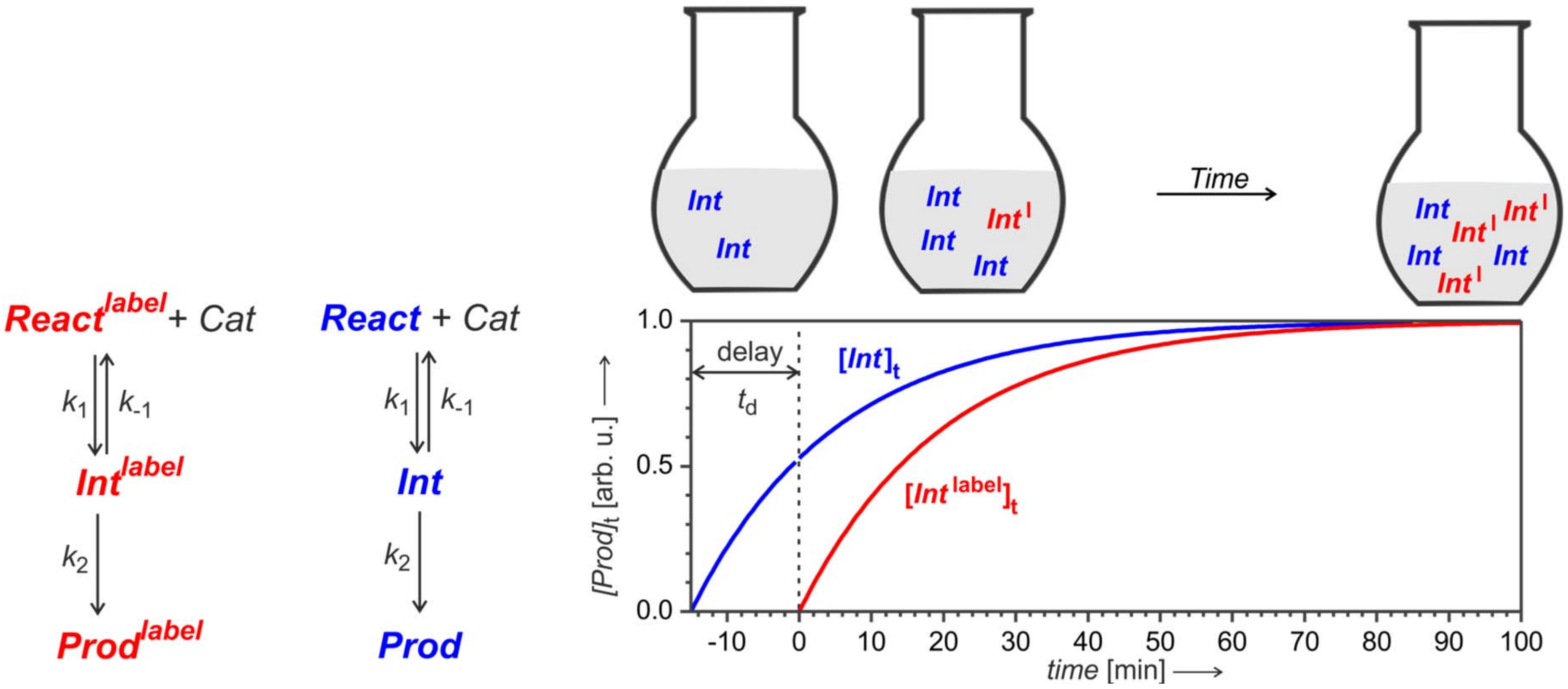

L. Jašíková, M. Anania, S. Hybelbauerová, J. Roithová, *J. Am. Chem. Soc.* **2015**, *137*, 13647.

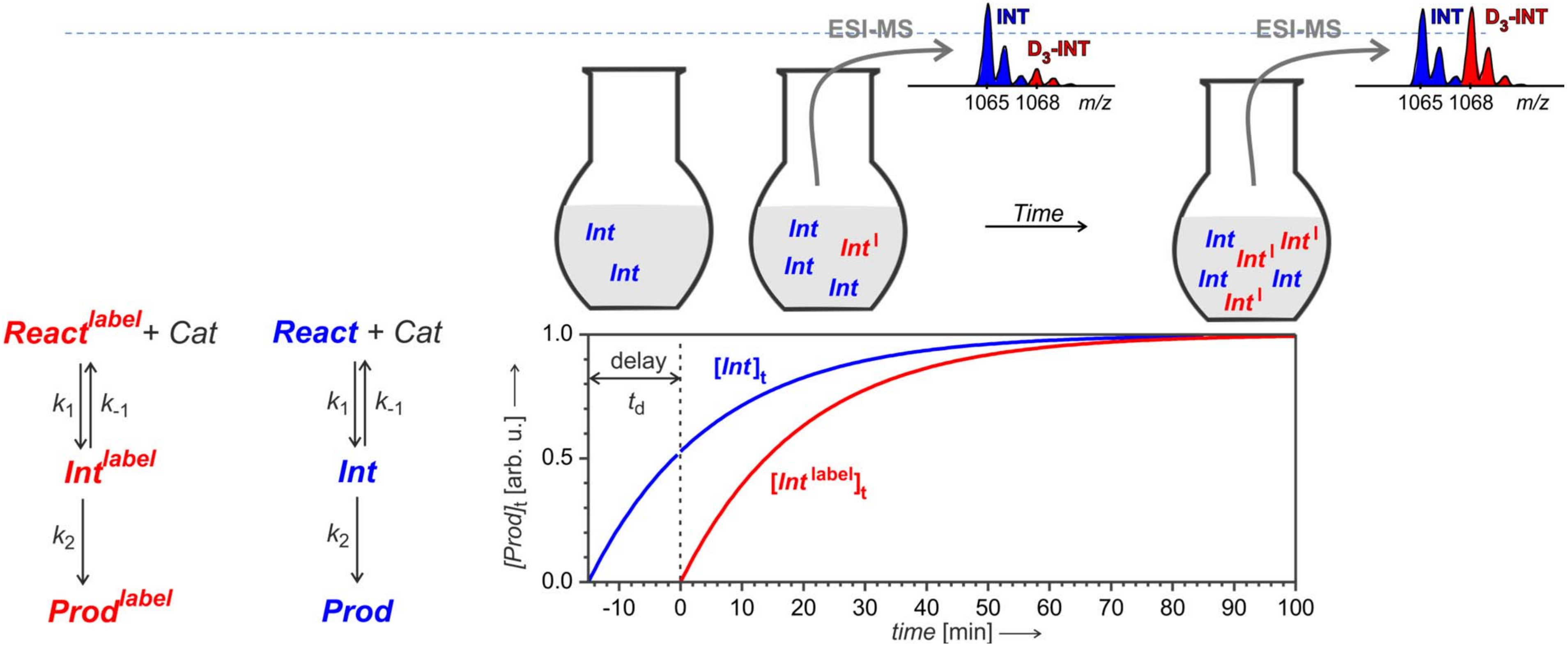

L. Jašíková, M. Anania, S. Hybelbauerová, J. Roithová, *J. Am. Chem. Soc.* **2015**, *137*, 13647.

$$\mathbf{React}^{label} + Cat \underset{k_{-1}}{\overset{k_1}{\rightleftharpoons}} \mathbf{Int}^{label} \xrightarrow{k_2} \mathbf{Prod}^{label}$$

$$\mathbf{React} + Cat \underset{k_{-1}}{\overset{k_1}{\rightleftharpoons}} \mathbf{Int} \xrightarrow{k_2} \mathbf{Prod}$$

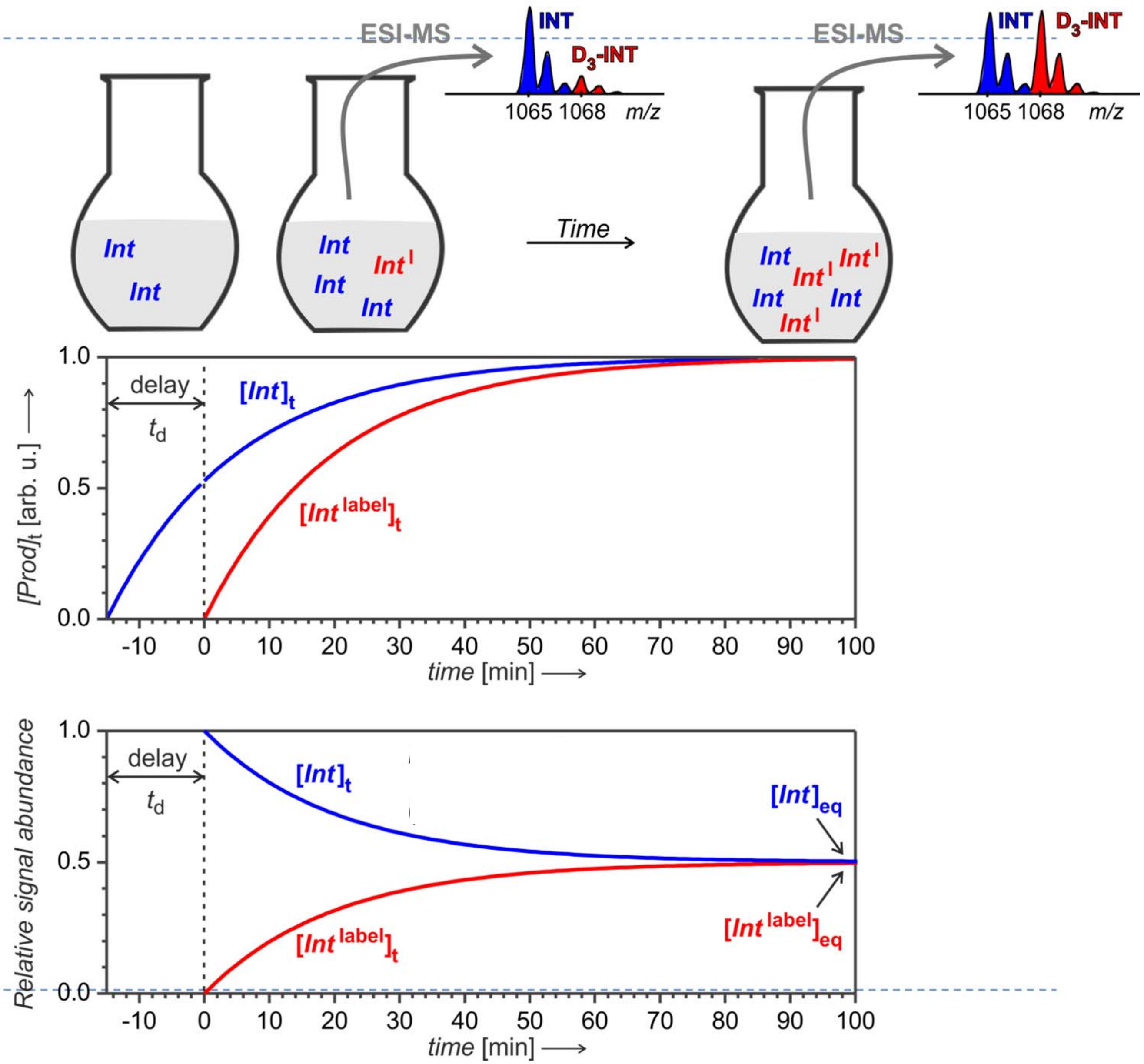

$$\begin{tikzcd}
\mathit{React}^{label} + \mathit{Cat} \arrow[d, shift right, "k_1"'] \\
\mathit{Int}^{label} \arrow[u, shift right, "k_{-1}"'] \arrow[d, "k_2"'] \\
\mathit{Prod}^{label}
\end{tikzcd}
\qquad
\begin{tikzcd}
\mathit{React} + \mathit{Cat} \arrow[d, shift right, "k_1"'] \\
\mathit{Int} \arrow[u, shift right, "k_{-1}"'] \arrow[d, "k_2"'] \\
\mathit{Prod}
\end{tikzcd}$$

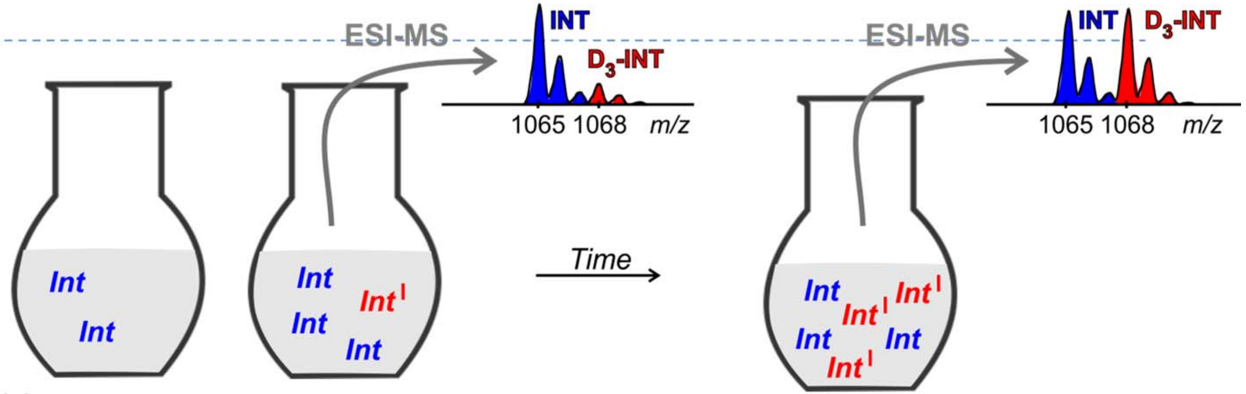

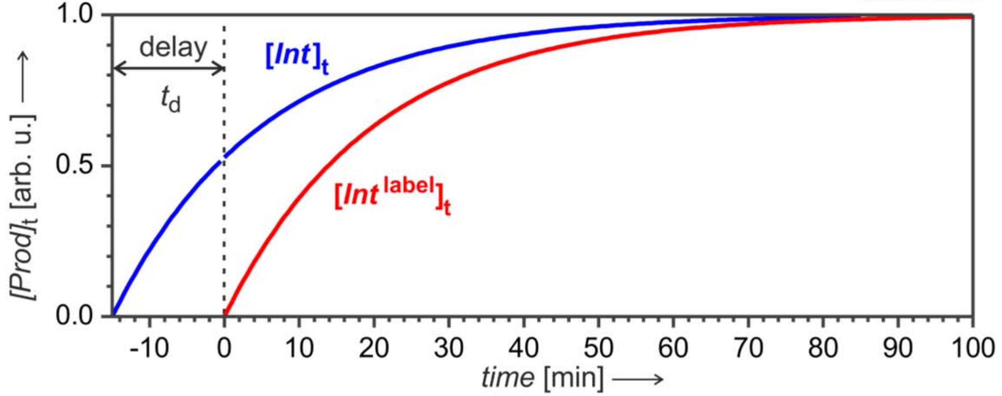

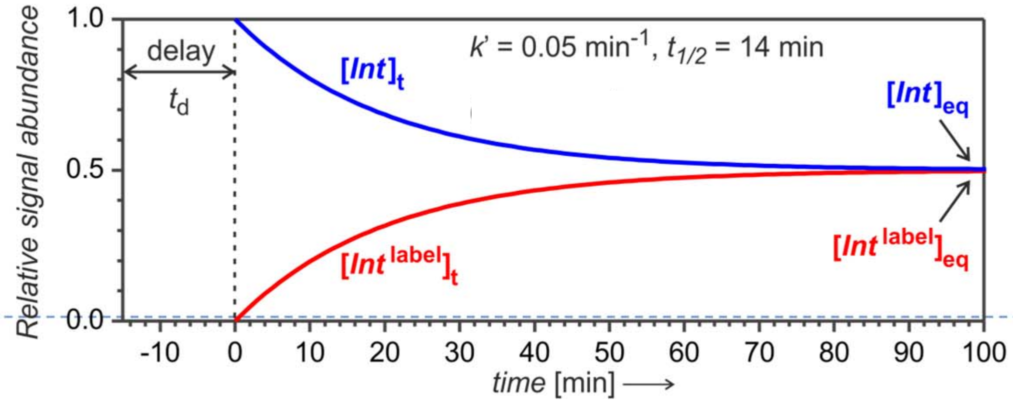

$$\left[\boldsymbol{Int}^{label}\right]_t = \left[\boldsymbol{Int}^{label}\right]_{eq}\left(\boldsymbol{1} - \boldsymbol{e}^{-k't}\right)$$

Kinetics of reaction intermediates

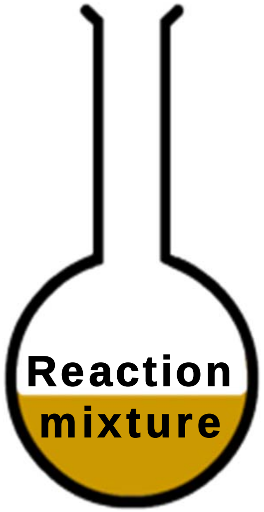

Ph-CC-CH_3
+ 2.5% [Au(PMe_3)Cl]
+ 3% $AgSbF_6$ in CH_3OH

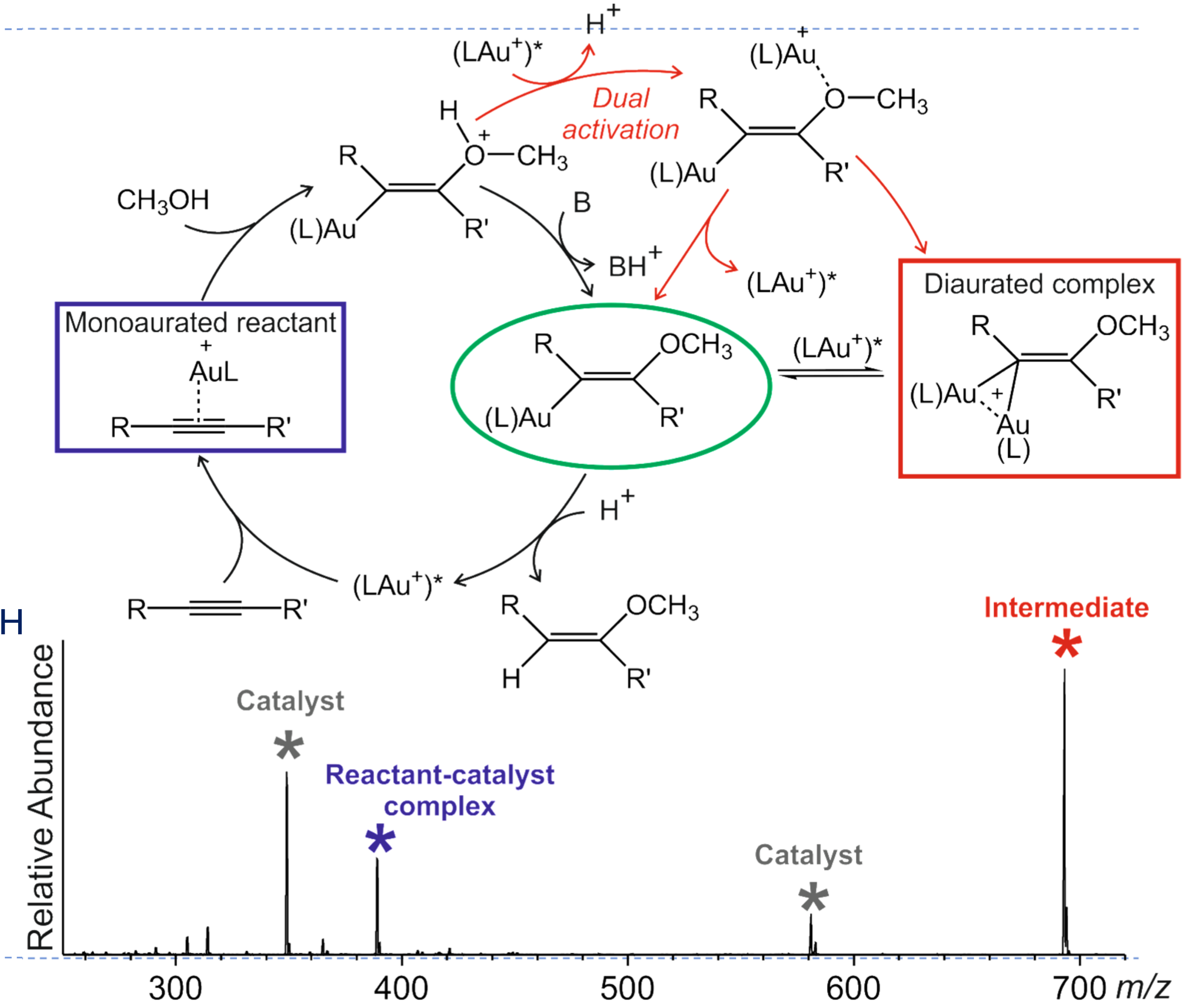

Effect of the ligand and the reaction conditions

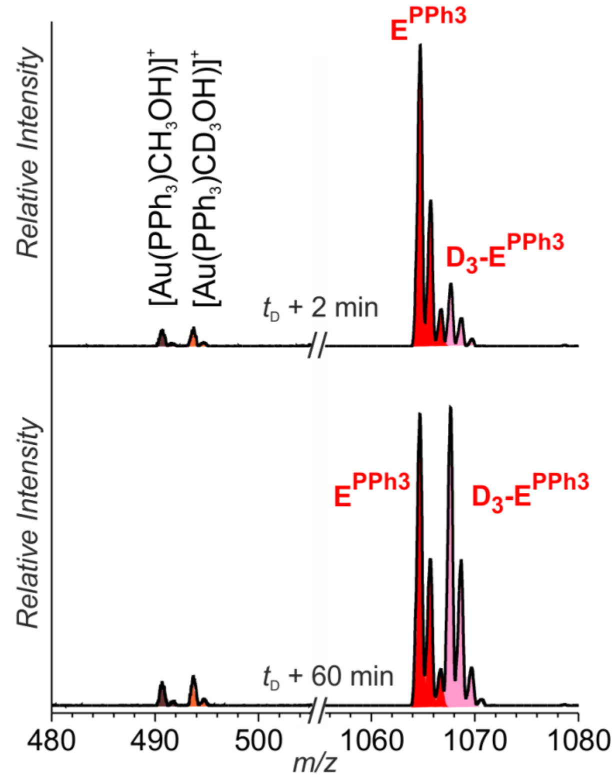

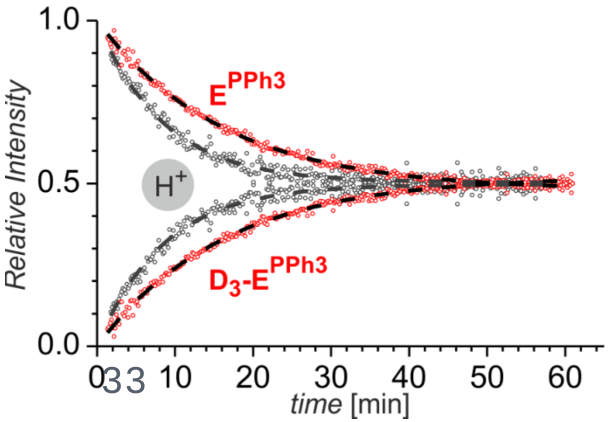

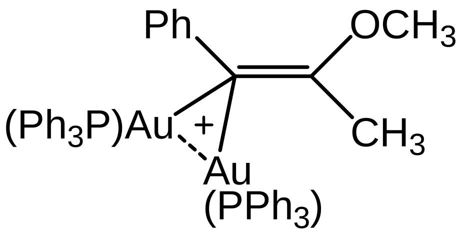

$t_{1/2}$ ~ 11 min

Catalyst	Addition	Additive	E^{PPh3} $t_{1/2}$ [min]
2.5 mol% [AuCl(PPh_3)]/ 3 mol% $AgSbF_6$	CD_3OH	-	11.3 ± 1.7
	CD_3OH	TsOH	7.0 ± 1.6
	$PhCCCH_3$,CD_3OH	-	7.3 ± 0.6
	$PhCCCH_3$,CD_3OH	TsOH	3.7 ± 0.3
	$PhCCCD_3$	-	4.2 ± 0.4
2.5 mol% [AuCl(PMe_3)]/ 3 mol% $AgSbF_6$	CD_3OD		4.0 ± 0.3[a]

Correlation with NMR kinetics

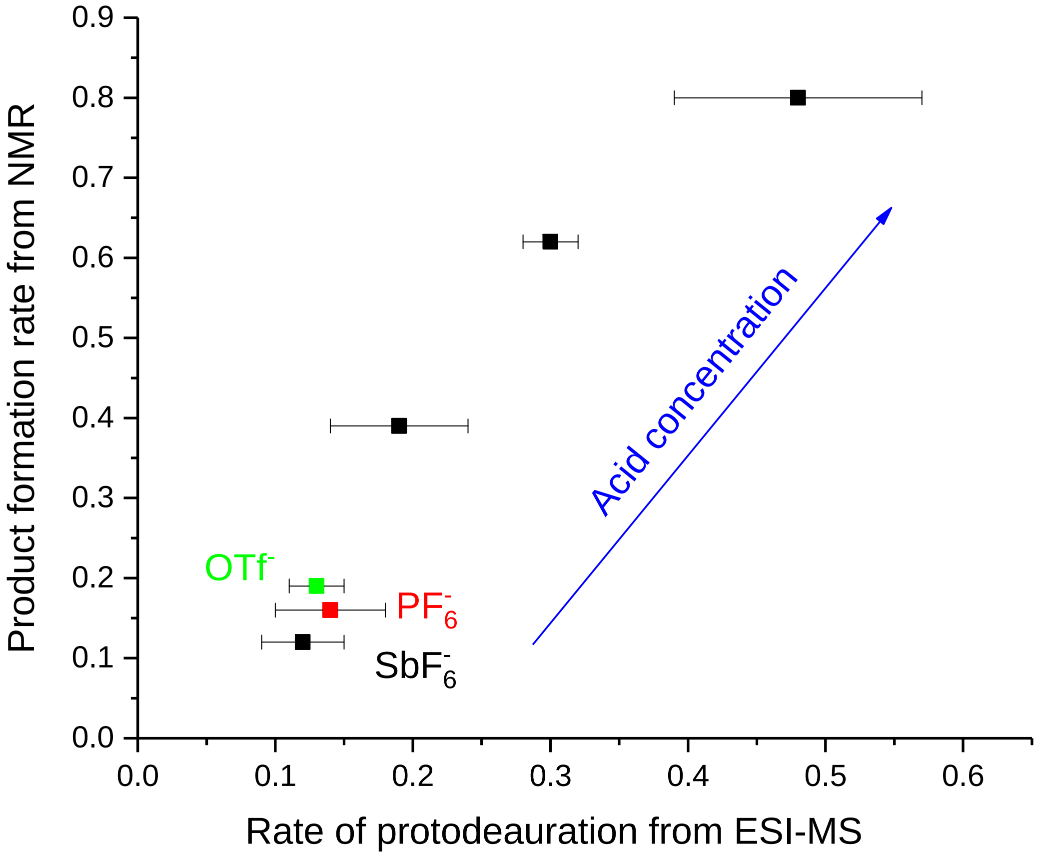

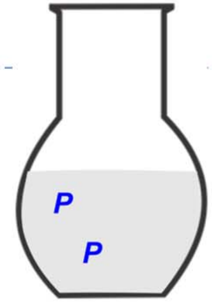

$$\mathbf{React} + \mathbf{R2} \underset{k_{-1}}{\overset{k_1}{\rightleftharpoons}} \mathbf{Int} \xrightarrow{k_2} \mathbf{Prod}$$

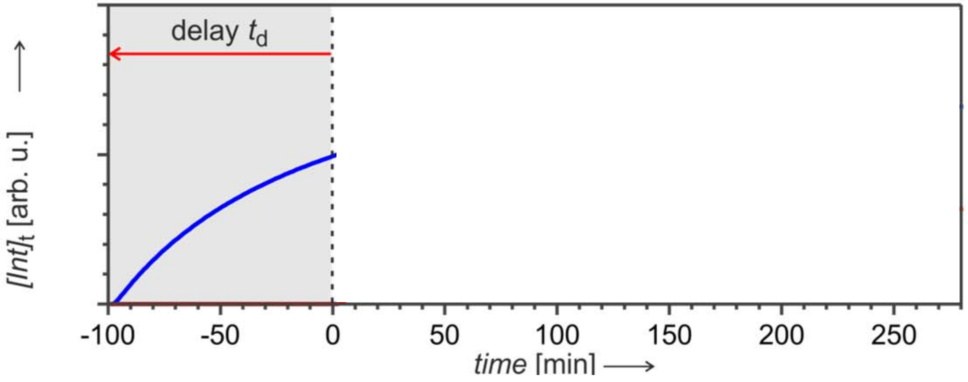

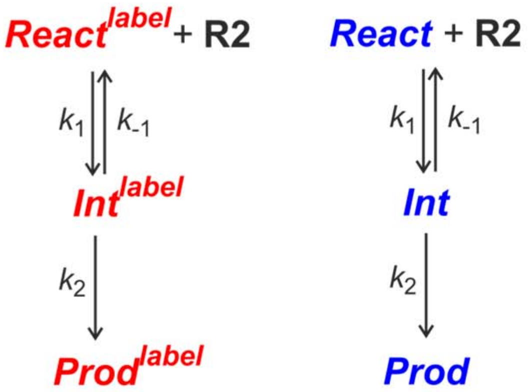
React^label + R2
k1
k-1
Int^label
k2
Prod^label
React + R2
k1
k-1
Int
k2
Prod

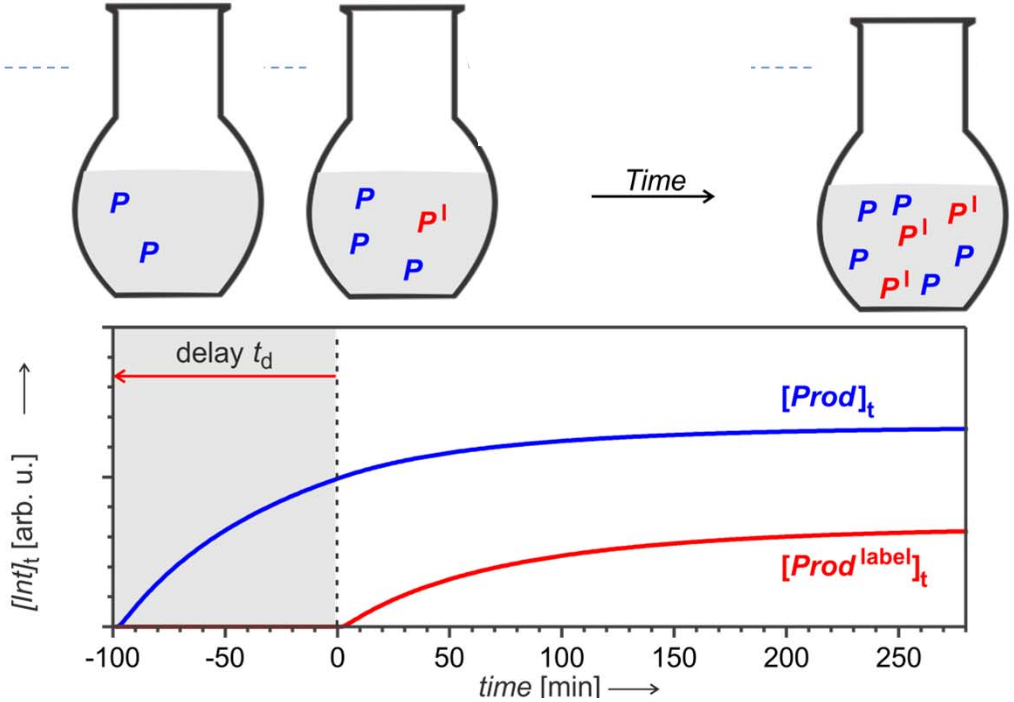
P
P
P
P
P
P^l
Time
P
P
P^l
P^l
P
P
P^l
P
delay t_d
[Prod]_t
[Prod^label]_t
[Int]_t [arb. u.]
-100
-50
0
50
100
150
200
250
time [min]

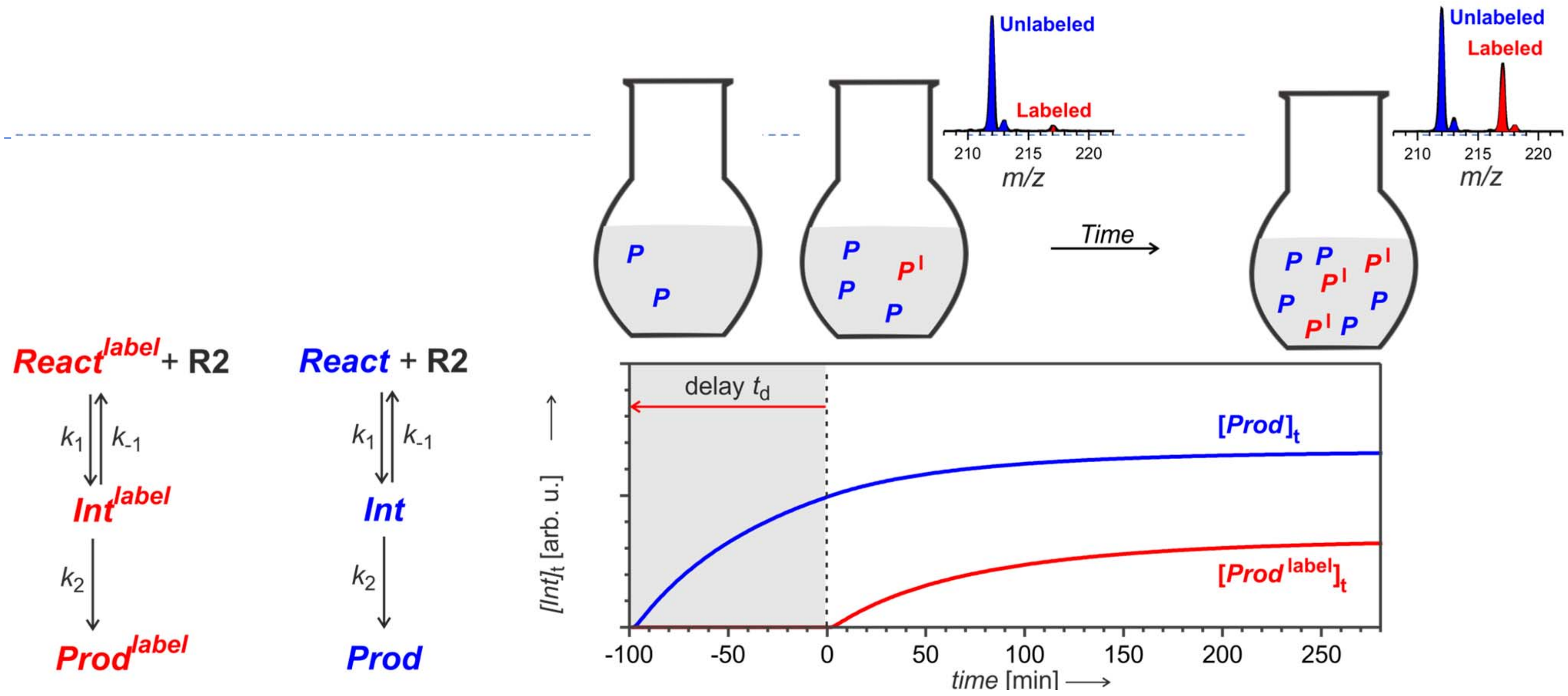

React^label + R2
k1
k-1
Int^label
k2
Prod^label
React + R2
k1
k-1
Int
k2
Prod
P
P
P
P^l
P
P
Unlabeled
Labeled
210
215
220
m/z
Time
P
P
P^l
P^l
P
P
P^l
P
Unlabeled
Labeled
210
215
220
m/z
delay t_d
[Prod]_t
[Prod^label]_t
[Int]_t [arb. u.]
-100
-50
0
50
100
150
200
250
time [min]

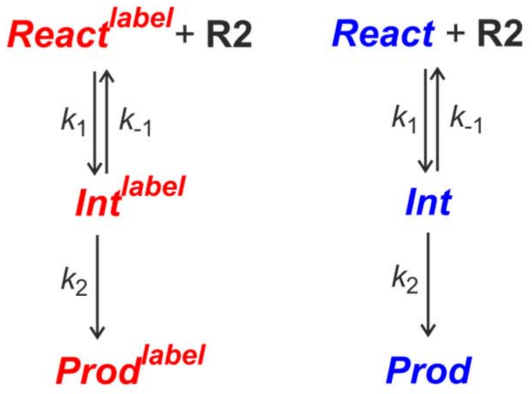
React^label + R2
k1
k-1
Int^label
k2
Prod^label
React + R2
k1
k-1
Int
k2
Prod

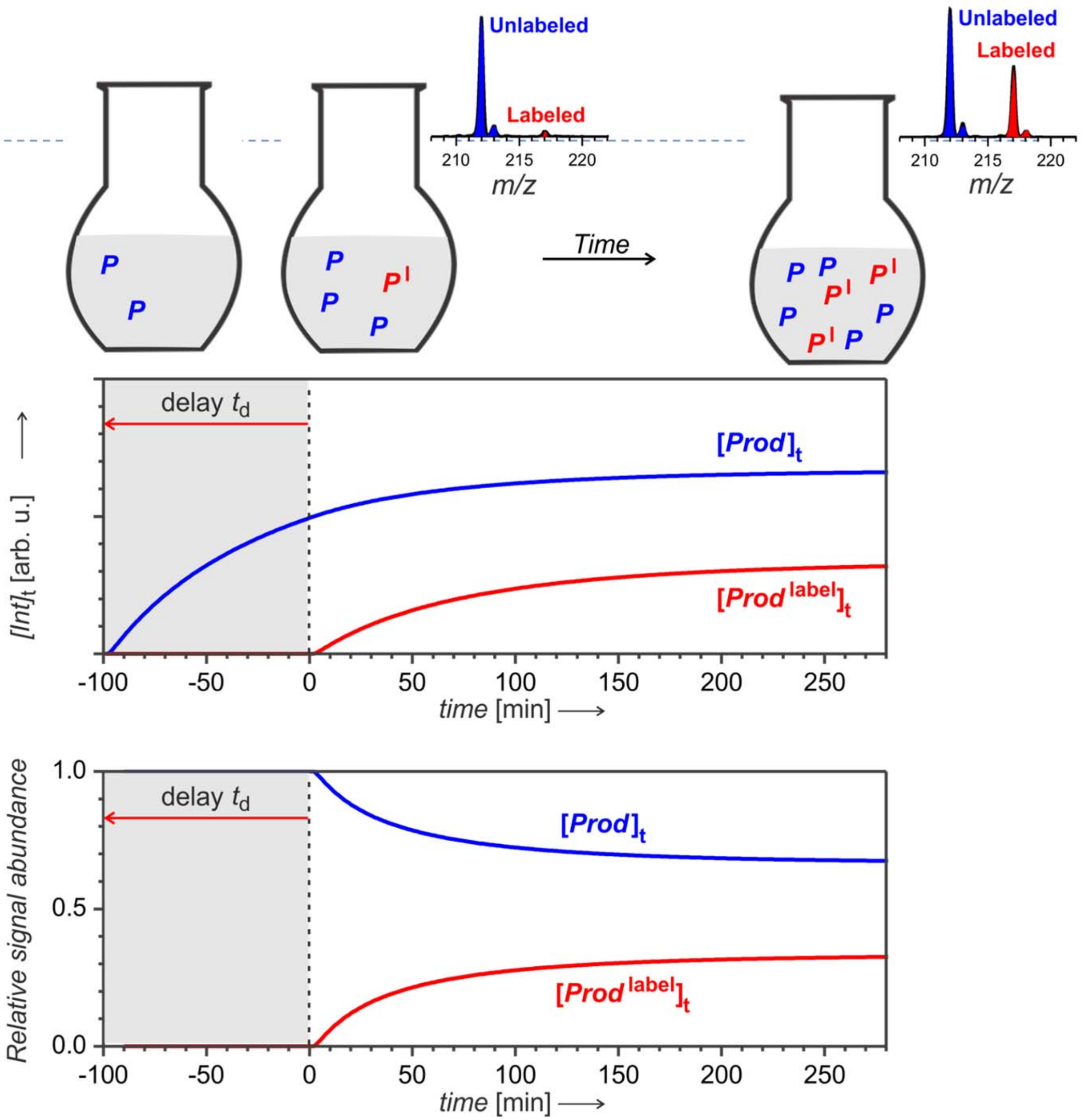
Unlabeled
Labeled
210
215
220
m/z
P
P
P
P
P
P^l
Time
P P P^l P^l P P P^l P
delay t_d
[Prod]_t
[Prod^label]_t
[Int]_t [arb. u.]
-100
-50
0
50
100
150
200
250
time [min]
Relative signal abundance
1.0
0.5
0.0

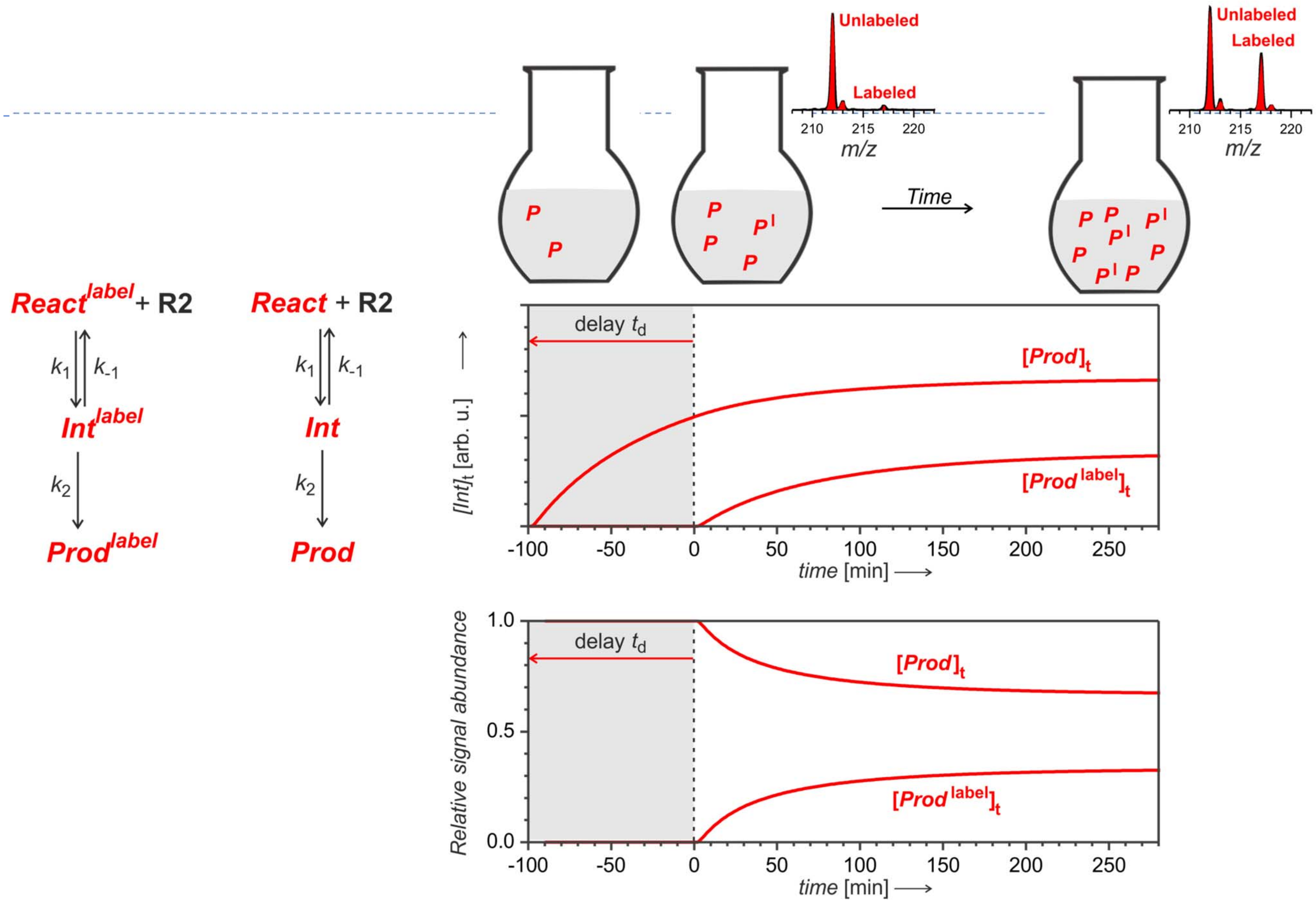
React^label + R2
k1
k-1
Int^label
k2
Prod^label
React + R2
k1
k-1
Int
k2
Prod
P
P
P
P^l
P
P
Unlabeled
Labeled
210
215
220
m/z
Time
P
P
P^l
P^l
P
P
P^l
P
Unlabeled
Labeled
210
215
220
m/z
delay t_d
[Prod]_t
[Prod^label]_t
[Int]_t [arb. u.]
-100
-50
0
50
100
150
200
250
time [min]
delay t_d
[Prod]_t
[Prod^label]_t
Relative signal abundance
1.0
0.5
0.0
-100
-50
0
50
100
150
200
250
time [min]

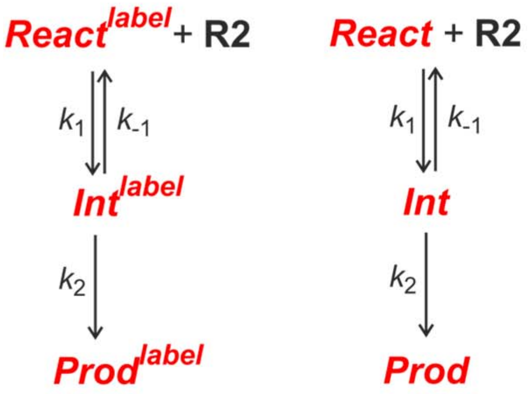

$$\begin{tikzcd} \text{React}^{label} + \text{R2} \arrow[d, shift right, "k_1"'] \\ \text{Int}^{label} \arrow[u, shift right, "k_{-1}"'] \arrow[d, "k_2"'] \\ \text{Prod}^{label} \end{tikzcd} \qquad \begin{tikzcd} \text{React} + \text{R2} \arrow[d, shift right, "k_1"'] \\ \text{Int} \arrow[u, shift right, "k_{-1}"'] \arrow[d, "k_2"'] \\ \text{Prod} \end{tikzcd}$$

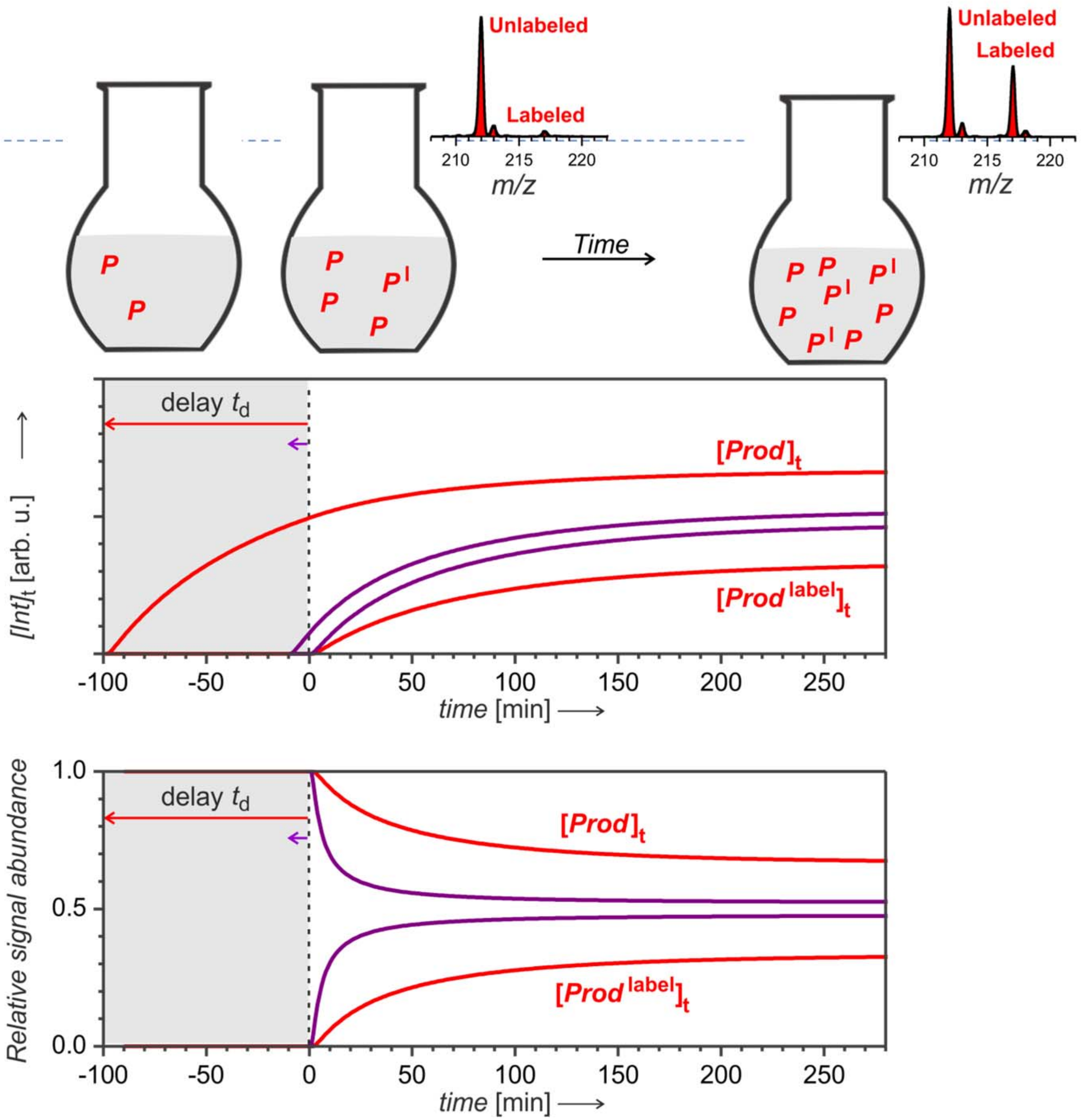

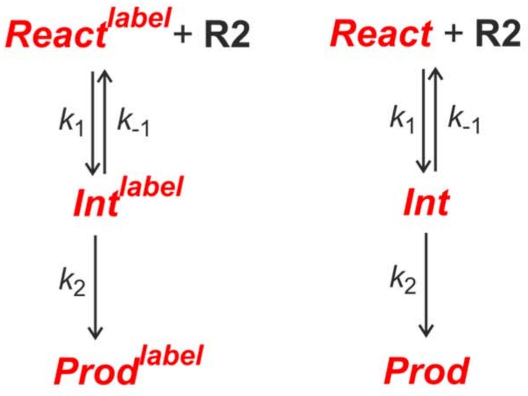
React^label + R2
k1
k-1
Int^label
k2
Prod^label
React + R2
k1
k-1
Int
k2
Prod

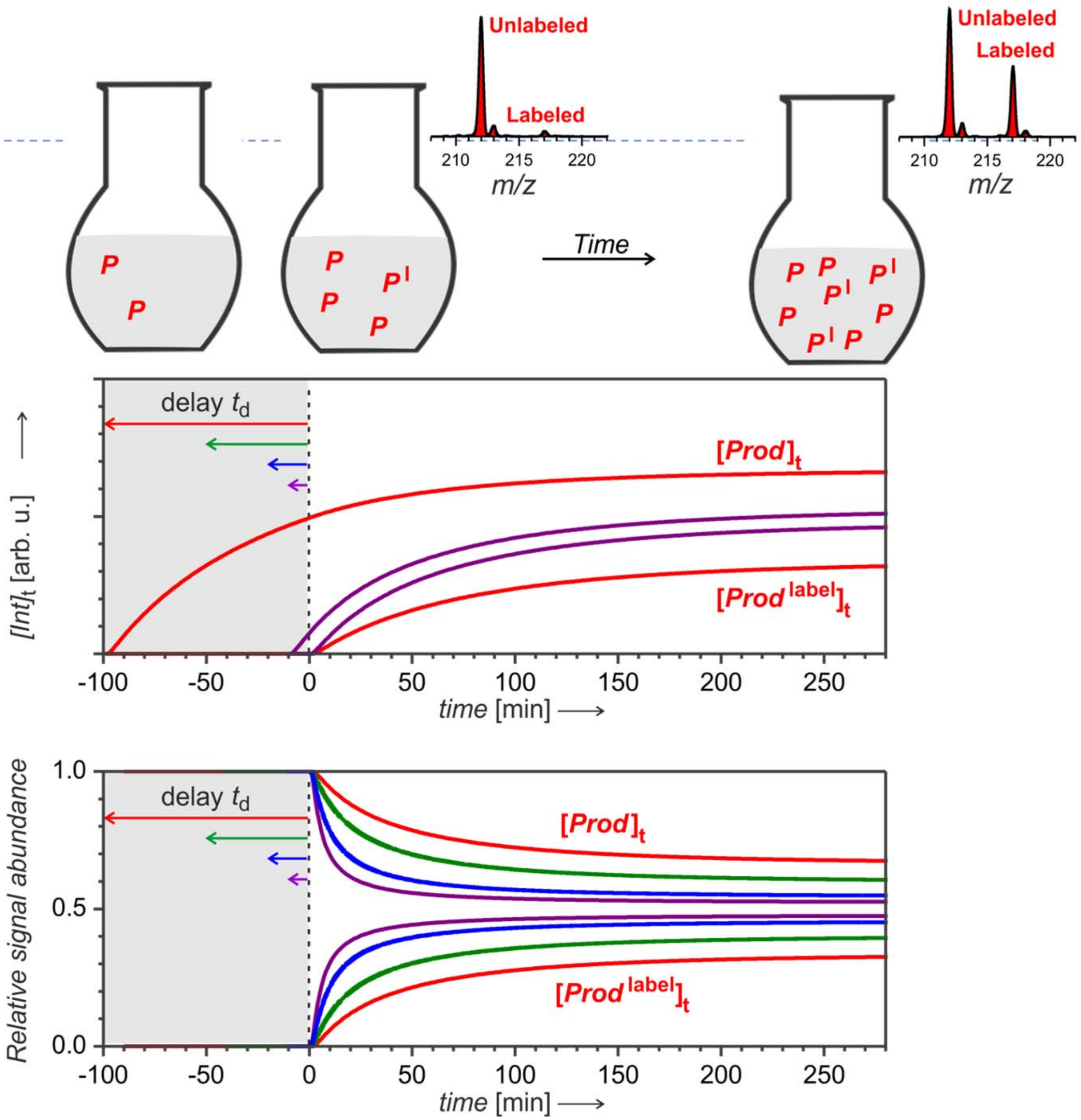
Unlabeled
Labeled
210
215
220
m/z
Unlabeled
Labeled
210
215
220
m/z
Time
P
P^l
delay t_d
[Prod]_t
[Prod^label]_t
[Int]_t [arb. u.]
-100
-50
0
50
100
150
200
250
time [min]
delay t_d
[Prod]_t
[Prod^label]_t
Relative signal abundance
1.0
0.5
0.0
-100
-50
0
50
100
150
200
250
time [min]

$[(IPr)_2Au_2(PhCCCH_3)(OCH_3)]^+$

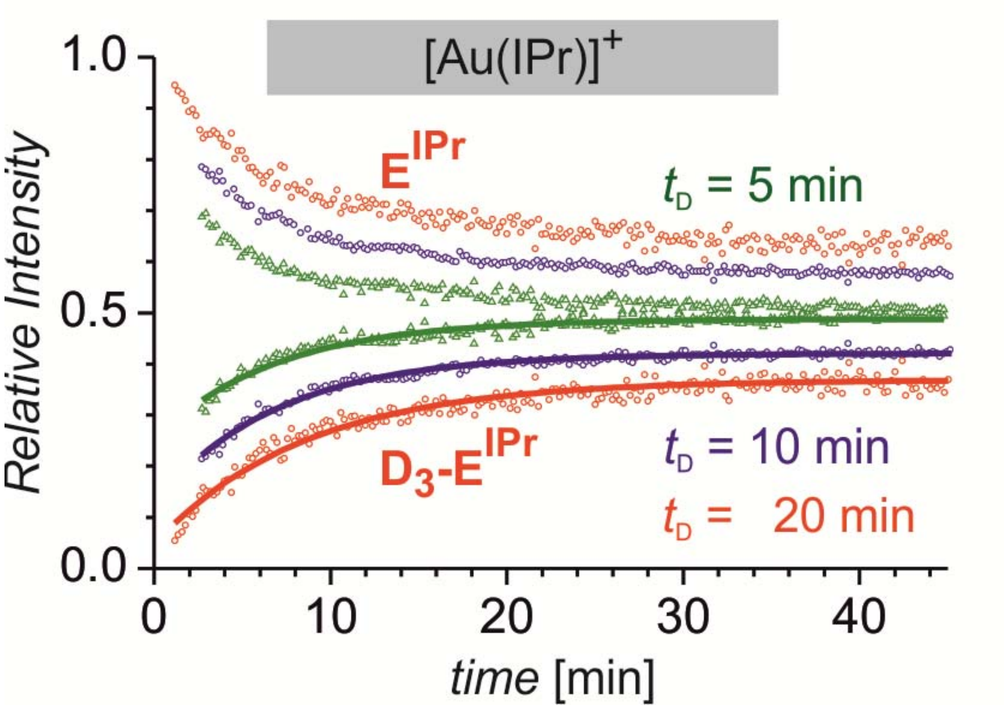

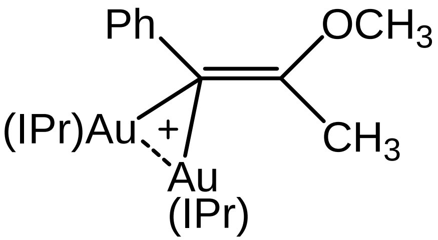

Reaction kinetics by MS

- Gas-phase
  - Tandem MS – QoQ and similar instruments
    - Barrier-less reactions, zero-collision energy, pressure dependence, rate constants by calibration, collisional (reaction) complex
  - Ion traps → reactions in time

- Reactions in condensed phase
  - Pressure gap, ion suppression, concentration changes – enrichment factors – speciation
  - Qualitative kinetics directly from ion current – all species similar with similar ionization/ion-transfer probability (sometimes even qualitatively correct)
  - Catalytic reactions – delayed reactant labeling, isotopic standards